

5. PLIOCENE-PLEISTOCENE CALCAREOUS NANNOFOSSILS FROM THE IBERIA ABYSSAL PLAIN¹

L. Liu,² P. Maiorano,³ and X. Zhao⁴

ABSTRACT

During Ocean Drilling Program Leg 149, five sites were drilled on the Iberia Abyssal Plain, west of the Iberian Peninsula. Five holes (Holes 897A, 897C, 898A, 899A, and 900A) yielded Pliocene-Pleistocene sediments, which consist mainly of turbidites. Among these, Holes 897C and 898A yielded significant Pliocene-Pleistocene sediments that provided a high-resolution nannofossil biostratigraphy essential for locating paleomagnetic polarity events and for interpreting the age and frequency of turbidite sedimentation in the Iberia Abyssal Plain.

Pliocene-Pleistocene nannofossils recovered during Leg 149 are generally abundant and well to moderately preserved. Although reworking is evident in most samples, the Pliocene-Pleistocene nannofossils proved quite reliable for dating the sediments. Most Pleistocene zonal boundaries proposed by S. Gartner in 1977 and the Pliocene standard zonal boundaries proposed by E. Martini in 1971 were easily recognized. In addition, several other nannofossil events proposed by D. Rio et al. in 1990 and by T. Sato and T. Takayama in 1992 were recognized and proved valuable for improving the resolution of Pliocene-Pleistocene nannofossil biostratigraphy.

The Pliocene-Pleistocene nannofossil biostratigraphic results of Holes 897C and 900A coincide rather well with the discerned paleomagnetic polarity events. As a result, the combination of nannofossil biostratigraphic and paleomagnetic studies provides important information for fulfilling the second objective of this leg: to determine the history of turbidite sedimentation in the Iberia Abyssal Plain.

The general trend of sedimentation rates inferred by nannofossil biostratigraphy indicates that sedimentation rates increase from the continental margin to the deep sea along with increasing water depth.

INTRODUCTION

During Ocean Drilling Program (ODP) Leg 149, five sites were drilled on the Iberia Abyssal Plain (Fig. 1). The principal objective was to sample the acoustic basement within the ocean/continent transition in order to establish its petrologic and physical nature. Another important goal was to discover the history of late Cenozoic turbidite sedimentation and determine to what extent the age and frequency of turbidites relate to past climatic change.

Of the eight holes drilled at five sites during Leg 149, Holes 897 A, 897C, 898A, 899A, and 900A yielded Pliocene-Pleistocene sediments that consist mainly of terrigenous turbidites, hemipelagites, and pelagites. The hemipelagic and pelagic layers situated at the top of most turbidite sequences provided abundant and well-preserved Pliocene-Pleistocene nannofossil assemblages. This study describes primarily the calcareous nannofossil assemblages and discusses the Pliocene-Pleistocene nannofossil biostratigraphy of Leg 149 (Table 1, Fig. 1).

In this study, in addition to most of the Pleistocene zonal boundaries of Gartner (1977) and the Pliocene standard zonal boundaries of Martini (1971), several other nannofossil events proposed by Rio et al. (1990a, 1990b), Sato and Takayama (1992), and Raffi et al. (1993) were recognized. This enabled us to provide a high-resolution nannofossil biostratigraphy, and thus to contribute essential age assignments to fulfill the second objective of this leg. In addition, this study

provided important information for locating paleomagnetic events (see Zhao et al., this volume).

METHODS

We selected our raw samples during the cruise by carefully examining each turbidite sequence indicated by sedimentary structures. Most samples were collected from the hemipelagic and pelagic layers situated at the top of the turbidite sequences in order to yield abundant and well-preserved Pliocene-Pleistocene nannofossil assemblages and to avoid severe reworking as far as possible. Smear slides were prepared directly from raw samples and were examined using phase contrast and polarized light microscopy to define the relative abundance of each nannofossil species present. A scanning electronic microscope (SEM) was employed to identify some biostratigraphically important species, such as *Emiliana huxleyi* and *Reticulofenestra asanoi*.

The relative abundance of individual species and the total abundance for each sample were tabulated on the distribution charts (Tables 2-9) using a light microscope with a magnification of $\times 1560$. The letters used on the range charts and the corresponding definitions are as follows:

R = rare (1 specimen per 51-200 fields of view);
F = few (1 specimen per 11-50 fields of view);
C = common (1 specimen per 2-10 fields of view);
A = abundant (1-10 specimens per field of view); and
V = very abundant (>10 specimens per field of view).

Lowercase letters are used to denote reworking.

The preservation of calcareous nannofossils was recorded as follows:

¹Whitmarsh, R.B., Sawyer, D.S., Klaus, A., and Masson, D.G. (Eds.), 1996. *Proc. ODP, Sci. Results*, 149: College Station, TX (Ocean Drilling Program).

²Department of Geology, Florida State University, Tallahassee, FL 32306, U.S.A.
li@geomag.gly.fsu.edu

³Department of Geology and Geophysics, Via E. Orabona, 4-70125, Bari, Italy.

⁴Institute of Tectonics, University of California, Santa Cruz, CA 95064, U.S.A.

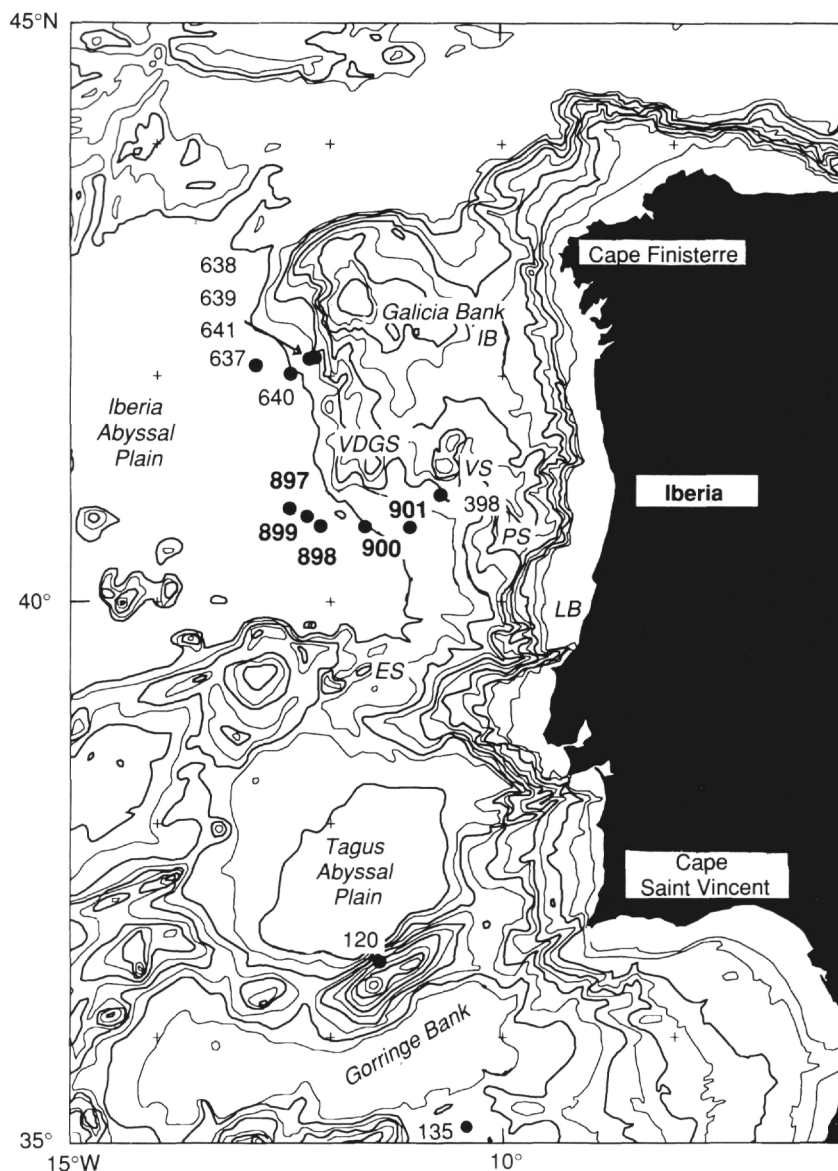


Figure 1. Location of Leg 149 drill Sites 897-901 and sites previously drilled by the Deep Sea Drilling Project and ODP.

- G = good; individual specimens exhibit little or no dissolution or overgrowth; diagnostic characteristics are preserved and nearly all of the specimens can be identified;
- M = moderate; individual specimens show evidence of dissolution or overgrowth; some specimens cannot be identified to the species level; and
- P = poor; individual specimens exhibit considerable dissolution or overgrowth.

Calcareous nannofossil species considered in this paper are listed in the Appendix, where they are arranged alphabetically by generic epithets. Bibliographic references for these taxa can be found in Perch-Nielsen (1985) and Sato and Takayama (1992).

ZONATION

Among several Pleistocene zonations proposed by Martini (1971), Bukry (1973, 1975), Gartner (1977), Okada and Bukry (1980), and Martini and Muller (1986), Gartner's zonal scheme, which recognizes seven zones within the Pleistocene, is the most

popular and was used in this study as the framework of our Pleistocene biostratigraphic zonation. In recent years, nannofossil workers have correlated the Pleistocene nannofossil events with oxygen isotope and paleomagnetic data in order to establish a more precise and detailed Pleistocene nannofossil zonal scheme for Zone NN19 (e.g., Pujos, 1985; Takayama and Sato, 1987; Matsuoka and Okada, 1989, 1990; Sato and Takayama, 1992; Raffi et al., 1993; Wei, 1993). The Pleistocene nannofossil events used in this paper (Table 1) combine the opinions of these authors.

The delineation of the Pliocene/Pleistocene boundary has long been controversial. Most nannofossil workers rely on the Martini (1971), Okada and Bukry (1980), or Gartner (1977) zonal schemes and therefore use the last occurrence (LO) of *Discoaster brouweri* to mark the Pliocene/Pleistocene boundary. However, with the acceptance of the Vrica section (Calabria, southern Italy) as the stratotype for the boundary, the Pliocene/Pleistocene boundary issue appears to have been resolved with the use of the first occurrence (FO) of *Gephyrocapsa oceanica* s.l. (approximately 1.6 Ma, above the Olduvai subchron) as the marker (Rio et al., 1990b). In this study, we used the FO of *Gephyrocapsa oceanica* s.l. to recognize the Pliocene/Pleistocene boundary.

Table 1. Pliocene-Pleistocene calcareous nannofossil biostratigraphic scheme.

		Zonation (Gartner, 1977)		Rio et al., 1990b		Nannofossil events in this study	
Pleistocene	NN21	<i>E. huxleyi</i> Acme Zone	} <i>E. huxleyi</i> acme	MNN21b	} <i>E. huxleyi</i> increase	NN21	
		<i>E. huxleyi</i> Zone		MNN21a			} <i>E. huxleyi</i>
	NN20	<i>G. oceanica</i> Zone	} <i>P. lacunosa</i>	MNN20	} <i>P. lacunosa</i>	NN20	
		<i>P. lacunosa</i> Zone		MNN19f			} <i>G. sp. 3</i>
	NN19b	small <i>Gephyrocapsa</i> Zone	} dominant small <i>Gephyrocapsa</i>	MNN19e	} large <i>Gephyrocapsa</i>	NN19	
		<i>H. sellii</i> Zone		MNN19d			} <i>H. sellii</i>
				MNN19c			
	NN19a	<i>C. macintyreii</i> Zone	} <i>C. macintyreii</i>	MNN19b	} <i>C. macintyreii</i>	NN19	
		Standard Zonation (Martini, 1971) (Martini and Müller, 1986)		} <i>D. brouweri</i>			MNN19a
	NN18		<i>D. brouweri</i> Zone		} <i>D. brouweri</i> <i>D. triradiatus</i>	NN18	
NN17		<i>D. pentaradiatus</i>	} <i>D. pentaradiatus</i> <i>D. surculus</i>	NN17			
	NN16	<i>D. surculus</i>			} <i>D. surculus</i>	MNN16b	} <i>D. tamalis</i>
NN15		<i>R. pseudoubilicus</i>	} <i>R. pseudoubilicus</i>	MNN16a			
	NN14	<i>D. asymmetricus</i>			} <i>D. asymmetricus</i>	MNN15	} <i>R. pseudoubilicus</i>
NN13		<i>C. rugosus</i>	} <i>C. rugosus</i>	MNN14			
	NN12	<i>A. tricorniculatus</i>			} <i>A. tricorniculatus</i>	MNN13	} <i>D. asymmetricus</i> FCO
				MNN12			

The Pliocene biostratigraphic zonation of Martini (1971) was followed in this study. Some modifications were necessary for the lower Pliocene: Zones NN14 and NN15 were always combined as previously suggested by Raffi and Rio (1979) and Rio et al. (1990b). The base of this interval was defined in this study by the FO of *Pseudoemiliana lacunosa*, instead of the FO of *Discoaster asymmetricus* as would be better estimated by quantitative analyses because *D. asymmetricus* appears to be absent from the lower part of its expected range. According to Lohman (1986) and Wei et al. (1988), the FO of *Pseudoemiliana lacunosa* approximates the *Discoaster asymmetricus* acme. For the uppermost Pliocene Zone NN19a, the definition of Zone MNN19a by Rio et al. (1990b) was followed.

The LO of *Triquetrorhabdulus rugosus* and the FO of *Ceratolithus acutus* are the best index events for the Miocene/Pliocene boundary (Cita and Gartner, 1973; Rio et al., 1990a). These marker species are not present in our samples, so the Miocene/Pliocene boundary is not recognized in the studied sites. The LO of *Discoaster quinqueramus* was used in this study to separate Miocene from Pliocene nannofossil assemblages. Above the LO of *D. quinqueramus*, the lowermost Pliocene biostratigraphic event in our material is represented by the FO of *Pseudoemiliana lacunosa*. A few samples between the FO of *P. lacunosa* and the LO of *D. quinqueramus* were placed with uncertainty in the lower Pliocene, but no biozone could

be identified. The lowermost Pliocene is missing in the four holes where Pliocene sediments were sampled.

HOLE SUMMARIES

Hole 897A

Only six cores were drilled from Hole 897A (40°50.32'N, 12°28.44'W, at a water depth of 5320.0 m), and all are of Pleistocene age. The turbidite sediments consist mainly of nannofossil ooze, nannofossil clay, silty clay and clayey silt, silt, and fine sand. Calcareous nannofossils are well preserved and abundant in most samples (Table 2).

Samples 149-897A-1R-1, 95-96 cm, to 1R-1, 125-126 cm, are assigned to the *Emiliana huxleyi* Zone (NN21), based on the FO of *Emiliana huxleyi*. The dominant species are *Calcidiscus leptoporus*, *Coccolithus crassipons*, *Gephyrocapsa* spp. (<3 µm), and *Reticulofenestra minuta*.

Samples 149-897A-3R-1, 39-40 cm, to 4R-1, 58-59 cm, are assigned to the *Gephyrocapsa oceanica* Zone (NN20), based on the absence of both *Emiliana huxleyi* and *Pseudoemiliana lacunosa*.

Samples 149-897A-4R-1, 128-129 cm, to 6R-5, 56-57 cm, are assigned to the NN19h Subzone in the *Pseudoemiliana lacunosa*

Table 2. Distribution of Pleistocene calcareous nannofossils, Hole 897A.

Age	Nannofossil zone	Hole 897A		Abundance	Preservation	<i>Calcidiscus leptoporus</i>	<i>C. macintyreii</i>	<i>Ceratolithus cristatus</i>	<i>Coccolithus crassispinus</i>	<i>C. pelagicus</i>	<i>Dictyococcites perplexa</i>	<i>D. productus</i>	<i>Discoaster</i> spp. (reworked)	<i>Emiliania huxleyi</i>	<i>Gephyrocapsa caribbeanica</i> (3–4 µm)	<i>G. oceanica</i> (3–4 µm)	<i>G. oceanica</i> (4–5.5 µm)	<i>G. spp.</i> (<3 µm)	<i>Helicosphaera carteri</i>	<i>H. sellii</i>	<i>Pontosphaera discopora</i>	<i>P. japonica</i>	<i>Pseudoemiliania lacunosa</i> (elliptical)	<i>P. lacunosa</i> (round)	<i>R. minuta</i> (<3 µm)	<i>R. minutula</i> (3–5 µm)	<i>Rhabdosphaera claviger</i>	<i>Scapholithus fossilis</i>	<i>Syracosphaera pulchra</i>	<i>Thoracosphaera</i> spp.	<i>Umbilicosphaera sibogae</i>		
		Core, section interval (cm)	Depth (mbsf)																														
Pleistocene	NN21	1R-1, 95–96	0.95	V	G	A	.	.	C	F	.	.	r	F	.	F	.	A	F	A	F	F	.	F	R	F			
		1R-1, 125–126	1.25	V	G	A	.	.	F	R	.	.	.	F	R	.	.	.	A	F	F	.	C	R	F	
	NN20	3R-1, 39–40	17.09	V	G	A	.	.	R	F	.	R	C	C	A	F	V	F	C	F	C	R	C		
		3R-1, 50–51	17.20	V	G	A	.	.	C	C	R	F	C	A	F	V	F	C	F	C	R	C		
		4R-1, 17–18	26.47	V	G	A	.	.	C	C	R	A	F	C	V	F	V	F	C	F	C	R	C		
		4R-1, 58–59	26.88	V	G	A	.	R	C	F	R	A	.	.	C	.	C	F	V	C	.	R	.	.	V	F	C	F	C	R	F		
	NN19	19h	4R-1, 128–129	27.58	V	G	A	r	.	C	F	R	V	.	C	.	C	F	V	C	.	.	.	A	C	V	C	R	F	C	R	F	
			4R-1, 135–136	27.65	V	G	A	.	.	F	F	R	A	.	.	C	.	C	F	V	C	.	F	R	A	C	V	C	R	F	C	R	F
			4R-2, 8–9	27.88	V	G	A	.	.	F	F	R	A	.	.	C	.	C	F	V	C	.	F	R	A	C	V	C	R	F	C	R	F
			4R-3, 92–93	30.22	V	G	A	.	R	R	.	R	.	V	.	C	.	C	F	C	F	.	R	.	A	C	C	F	F	C	R	R	
			4R-3, 139–140	30.69	V	G	A	.	R	R	.	R	.	.	.	C	.	C	F	V	C	.	R	R	A	C	A	F	C	F	C	R	C
			4R-CC	36.00	V	G	A	.	.	C	R	.	V	.	.	C	.	C	F	A	F	.	R	.	A	F	A	F	F	F	F	R	F
			5R-1, 148–149	37.48	V	G	A	.	.	C	R	.	V	.	.	C	.	C	F	A	F	r	R	.	A	F	A	F	F	F	F	R	F
			5R-2, 21–22	37.71	V	G	A	.	.	C	R	R	V	.	.	C	.	C	F	A	F	.	R	.	A	F	A	F	F	F	F	R	F
			5R-2, 46–47	37.96	V	G	A	.	.	F	R	.	V	.	.	C	.	C	F	A	C	.	R	.	A	C	A	F	C	F	F	R	F
			5R-2, 80–81	38.30	V	G	A	.	.	F	.	.	V	.	.	C	.	C	F	A	F	.	R	.	A	C	A	F	F	F	F	R	F
			5R-2, 136–137	38.86	V	G	A	.	.	F	.	.	V	.	.	C	.	C	F	A	F	.	R	.	A	C	A	F	F	.	F	R	.
			5R-3, 11–12	39.11	V	G	C	.	R	F	R	V	.	.	F	F	V	F	F	F	V	.	F	R	C	F	V	.	R	.	F	R	F
			5R-3, 32–33	39.32	V	G	A	.	.	R	R	.	A	.	.	C	.	C	F	V	F	.	F	R	A	F	V	.	F	.	F	R	C
			5R-CC	45.60	V	G	A	.	.	F	R	.	A	.	.	C	.	C	C	A	F	.	F	.	A	C	A	A	R	F	R	F	R
			6R-1, 92–93	46.52	V	G	C	.	.	F	R	C	.	.	.	C	.	C	F	V	F	.	F	R	A	F	V	C	F	.	F	R	R
			6R-2, 68–69	47.78	V	G	C	.	.	C	F	.	V	.	.	C	.	C	F	A	F	.	R	R	A	F	A	C	F	.	F	R	F
			6R-3, 47–48	49.07	V	G	A	.	R	R	R	R	A	.	.	C	.	C	R	V	F	.	R	R	A	C	A	C	F	F	F	R	F
			6R-4, 150–151	51.60	V	G	A	.	.	F	R	.	A	r	.	C	.	C	R	A	F	.	R	.	C	R	A	A	R	.	R	R	R
	6R-5, 5–6	51.65	V	G	A	.	.	F	R	.	V	.	.	C	.	C	F	A	F	.	R	.	.	C	C	R	R	R	R	F			
	6R-5, 56–57	52.16	V	G	A	.	.	F	F	.	A	r	.	C	.	C	F	C	F	.	R	.	C	R	C	A	F	R	F	R	F		

Note: V = very abundant; A = abundant; C = common; F = few; R = rare; G = good; M = moderate; P = poor; r = rare (reworked).

Zone (NN19), based on the co-occurrence of *Pseudoemiliania lacunosa* and *Gephyrocapsa oceanica* s.l. (>4 µm) and the absence of *Reticulofenestra asanoi* (>6.5 µm), large *Gephyrocapsa* (>5.5 µm), and *Helicosphaera sellii*.

Hole 897C

The Pliocene-Pleistocene sediments from Hole 897C (40°50.33'N, 12°28.44'W, at a water depth of 5315.2 m) consist mainly of nannofossil ooze, nannofossil clay, silty clay and clayey silt, silt, and fine sand. Calcareous nannofossils are well preserved and abundant in most of the samples (Tables 3, 4).

The first *Gephyrocapsa oceanica* s.l. was found in Sample 149-897C-14R-3, 14–15 cm. Therefore, Samples from 149-897C-1R-1, 45–46 cm, to 14R-3, 14–15 cm, are assigned to the Pleistocene. Samples from 149-897C-14R-4, 88–89 cm, to 27R-1, 5–6 cm, are assigned to the Pliocene.

Pleistocene

All of the Pleistocene samples from Hole 897C are assigned to the *Pseudoemiliania lacunosa* Zone (NN19), based on the co-occurrence of *Pseudoemiliania lacunosa* and *Gephyrocapsa oceanica* s.l. (>4 µm).

Additional events used to further subdivide the *Pseudoemiliania lacunosa* Zone are recognized as the following:

1. LO of *Reticulofenestra asanoi* (>6.5 µm): Sample 149-897C-8R-2, 105–106 cm.

2. Reoccurrence of *Gephyrocapsa oceanica* (>3 µm), which corresponds to the FO of *Gephyrocapsa* sp. C-D of Matsuoka and Okada (1990): Sample 149-897C-8R-3, 58–59 cm.
3. FO of *Reticulofenestra asanoi* (>6.5 µm): Sample 149-897C-9R-CC.
4. LO of large *Gephyrocapsa* (>5.5 µm), which corresponds to the LO of *Gephyrocapsa* sp. A-B of Matsuoka and Okada (1990): Sample 149-897C-11R-2, 18–19 cm.
5. LO of *Helicosphaera sellii*: Sample 149-897C-11R-2, 18–19 cm.
6. FO of large *Gephyrocapsa* (>5.5 µm): Sample 149-897C-12R-5, 133–134 cm.
7. LO of *Calcidiscus macintyreii*: Sample 149-897C-14R-3, 14–15 cm.
8. FO of *Gephyrocapsa oceanica* s.l. (>4 µm): Sample 149-897C-14R-3, 14–15 cm.

Pliocene

Samples 149-897C-17R-2, 80–81 cm, to 14R-4, 88–89 cm, are placed within the uppermost Pliocene Zone NN19a, based on the absence of both *Discoaster brouweri* and *Gephyrocapsa oceanica* s.l. (>4 µm). The assemblage is also characterized by *Calcidiscus leptoporus*, *Calcidiscus macintyreii*, *Gephyrocapsa caribbeanica*, *Gephyrocapsa* sp., small *Gephyrocapsa*, *Helicosphaera acuta*, *Helicosphaera carteri*, and *Helicosphaera sellii*. It is noteworthy that the lowest occurrence of *Helicosphaera acuta* is peculiar in our sites: the species always occurs with the LO of *Discoaster surculus* or slightly above.

Table 3. Distribution of Pleistocene calcareous nannofossils, Hole 897C.

Age	Nannofossil zone	Hole 897C		Abundance	Preservation	Fossil Species																															
		Core, section, interval (cm)	Depth (mbsf)			<i>Calcidiscus leptorhus</i>	<i>C. macintyrei</i>	<i>Ceratolithus cristatus</i>	<i>Coccolithus erasipons</i>	<i>C. pelagicus</i>	<i>Diacyclopsites perplexa</i>	<i>D. productus</i>	<i>Discoaster</i> spp. (reworked)	<i>Gephyrocapsa caribbeatica</i> (3-4 µm)	<i>G. caribbeatica</i> (4-5.5 µm)	<i>G. caribbeatica</i> (>5.5 µm)	<i>G. oceanica</i> (3-4 µm)	<i>G. oceanica</i> (4-5.5 µm)	<i>G. oceanica</i> (>5.5 µm)	<i>G. spp.</i> (<3 µm)	<i>Helicosphaera carteri</i>	<i>H. sellii</i>	<i>Pontosphaera discopora</i>	<i>P. japonica</i>	<i>Pseudoemiliania lacunosa</i> (elliptical)	<i>P. lacunosa</i> (round)	<i>Reticulofenestra asanoi</i> (>6 µm)	<i>R. minuta</i>	<i>R. minutula</i>	<i>R. sp. A</i>	<i>Rhabdosphaera claviger</i>	<i>Scapholithus fossilis</i>	<i>Syracosphaera pulchra</i>	<i>Thoracosphaera</i> spp.	<i>Unibulbosphaera sibogae</i>		
Pleistocene	NN19	19h	1R-1, 45-46	50.35	V	G	A	.	F	F	.	A	.	C	.	A	R	.	V	F	.	.	A	C	.	V	C	.	R	R	F	R	R				
			1R-1, 98-99	50.88	V	G	A	.	F	R	.	A	r	C	.	.	A	F	.	A	F	.	.	A	F	.	A	C	.	F	.	R	R	R			
			1R-2, 7-8	51.47	V	G	A	.	.	R	.	A	C	C	.	V	F	.	R	.	A	C	.	C	C	.	R	C	F	R	F		
			1R-3, 68-69	53.58	V	G	A	.	.	R	R	R	C	.	C	.	.	C	C	.	V	F	.	F	.	A	C	.	A	C	.	R	R	R	R	F	
			2R-1, 69-70	60.59	V	G	C	.	.	F	R	R	A	r	C	.	.	A	.	.	A	F	.	.	R	R	.	A	C	.	R	R	R	R	R		
			2R-1, 128-129	61.18	V	G	C	.	.	R	R	.	V	.	A	.	.	A	.	.	A	R	.	.	R	R	.	A	A	.	R	.	F	R	R		
			3R-1, 53-54	70.13	V	G	C	.	.	R	R	.	A	.	A	.	.	A	.	.	A	F	.	R	F	R	.	A	A	.	R	.	R	.	.		
			3R-1, 84-85	70.44	A	G	C	.	.	R	R	.	A	r	C	.	.	A	.	.	C	F	.	.	R	R	.	A	A	.	.	.	R	R	.		
			4R-1, 14-15	79.34	V	G	A	.	.	R	R	.	V	.	A	.	.	A	.	.	A	C	.	F	.	A	C	.	C	C	.	F	R	C	R	F	
			5R-1, 80-81	89.70	A	G	C	.	R	C	C	.	C	r	F	.	.	C	.	.	C	.	R	F	R	C	F	.	A	F	
		5R-2, 60-61	91.00	A	G	A	.	C	C	.	C	r	F	.	.	.	C	.	.	C	F	.	.	C	C	.	A	C	.	R	.	F	R	F	.		
		6R-1, 48-49	98.98	A	G	C	.	.	F	C	R	C	.	C	.	.	C	.	.	A	F	R	R	.	A	F	.	A	F	.	.	C	F	R	.		
		7R-1, 106-107	109.26	V	G	A	.	.	F	R	.	C	.	C	.	.	C	R	.	A	F	.	R	.	A	C	.	A	F	.	F	.	F	R	F		
		8R-2, 105-106	120.45	V	G	A	A	F	.	A	F	.	F	R	A	C	C	V	A	C	F	.	R	R	F		
		8R-3, 58-59	121.48	V	G	A	A	F	.	A	F	.	R	.	A	C	A	A	A	A	F	.	R	R	F		
		8R-CC	127.50	A	G	A	.	.	R	A	F	.	R	.	A	F	A	A	A	C	.	R	R	R	.		
		9R-1, 29-30	127.79	V	G	A	A	F	.	.	A	F	A	A	V	A	R	.	R	.	R	.		
		9R-2, 2-3	129.02	A	G	A	.	.	R	R	R	.	.	C	F	F	.	A	F	R	R	.	R	.	R	.		
		9R-CC	137.20	V	G	A	.	R	R	A	R	.	.	C	F	F	A	A	F	R	.	.	R	.	R	.	R	.		
		19e	10R-1, 102-103	138.22	A	G	A	.	R	R	F	R	A	F	.	R	.	A	C	.	A	A	.	F	R	.	R	F	.	F		
		19d	10R-2, 34-35	139.04	V	G	A	.	R	R	.	.	.	R	A	F	.	.	A	C	.	A	A	.	F	R	F	R	R	.	R	.	
		19d	11R-2, 18-19	147.27	V	G	A	.	F	R	C	.	r	C	.	C	C	C	A	F	R	R	.	A	C	.	A	A	.	R	.	R	R	R	.	R	
		19d	11R-3, 10-11	148.40	V	G	A	.	F	R	C	.	.	C	.	C	C	C	F	C	F	V	C	R	F	R	V	C	.	A	C	.	C	R	R	R	
		19d	11R-4, 88-89	150.68	V	G	A	.	R	F	R	C	.	.	C	.	C	F	.	C	F	C	F	F	R	.	A	C	.	C	C	.	F	.	R	R	
		19d	11R-CC	156.60	A	G	C	.	.	F	F	C	.	r	C	.	C	F	.	C	F	.	C	F	A	C	F	F	.	A	F	.	A	C	.	F	.
		19d	12R-2, 4-5	158.14	A	G	A	.	F	R	F	F	.	F	F	F	F	F	F	F	F	F	F	F	A	F	.	F	R	A	C	.	A	C	.	F	.
		19d	12R-3, 125-126	160.85	A	G	A	.	F	R	F	F	r	F	F	F	F	F	F	F	F	F	F	F	A	F	.	R	.	A	C	.	A	C	F	R	F
		19d	12R-5, 133-134	163.93	V	G	A	.	R	.	A	C	.	C	.	C	F	.	C	F	V	F	F	F	.	A	C	.	A	F	.	F	R	F	R	.	
		19c	12R-6, 133-134	165.43	A	G	C	.	.	F	F	C	F	.	C	.	.	C	.	.	R	.	R	.	C	C	.	A	.	.	R	.	R	.	R	.	
		19c	14R-1, 46-47	176.26	A	G	A	.	C	F	C	C	r	C	C	.	C	C	.	.	R	.	R	.	C	F	.	A	A	
19b	14R-2, 79-80	178.09	V	G	A	.	.	C	F	C	A	C	C	.	C	C	.	V	C	C	.	.	A	F	.	C	F	.	F	R	F	R	.	.			
19b	14R-3, 14-15	178.94	V	G	A	R	.	R	R	.	A	r	C	F	.	C	F	.	C	R	F	.	C	F	.	C	A	.	R	.	R	R	.	.			

Note: V = very abundant; A = abundant; C = common; F = few; R = rare; G = good; M = moderate; P = poor; r = rare (reworked).

Zone NN18 (*Discoaster brouweri* Zone) is recognized from Samples 149-897C-23R-1, 113-114 cm, to 17R-3, 17-18 cm, based on the presence of *Discoaster brouweri* and *Discoaster triradiatus*. The assemblage is characterized by rare to abundant *Gephyrocapsa* spp. (<3 µm), rare to common *Helicosphaera acuta*, common to few *Helicosphaera sellii* and *Helicosphaera carteri*, and abundant to common *Pseudoemiliania lacunosa*.

Samples 149-897C-25R-CC, 5-6 cm, to 23R-2, 88-89 cm, are tentatively assigned to Zone NN17 (*Discoaster pentaradiatus* Zone). *Discoaster pentaradiatus* should characterize the zone, but the species is rare and sporadic, as it is also in the *Discoaster surculus* Zone. We choose to recognize the top of the zone above the relatively continuous range of the species. Reworked specimens of *Discoaster asymmetricus*, *Discoaster tamalis*, and *Discoaster surculus* are recorded in the same interval as are rare occurrences of *Discoaster pentaradiatus* so it is possible that these are reworked. The assemblage is common to abundant, with moderate to good preservation.

Zone NN 16 (*Discoaster surculus* Zone) is recognized from Samples 149-897C-26R-1, 93-94 cm, to 26R-1,4-5 cm, based on the absence of *Reticulofenestra pseudumbilicus* and the presence of *Discoaster surculus*. *Discoaster brouweri*, *Discoaster pentaradiatus*, and *Discoaster triradiatus* are also recorded within this zone, as is the highest occurrence of *Discoaster asymmetricus* and *Discoaster tamalis*; *Helicosphaera acuta* is present in the uppermost part of the zone.

Samples 149-897C-26R-2, 108-109 cm, to 26R-2, 6-7 cm, are placed within the combined lower Pliocene Zones NN14-15. The FO of *Pseudoemiliania lacunosa* and the LO of *Reticulofenestra pseudumbilicus* are used to define this interval.

Samples 149-897C-27R-1, 5-6 cm, to 27R-1, 1-2 cm, are placed in the lowermost Pliocene but no biozone can be recognized. *Amaurolithus delicatus* and *Discoaster tamalis* are recorded within this zone.

Hole 898A

Hole 898A (41°41.100'N, 127°3.380'E, at a water depth of 5279.0 m) is the only hole that was drilled with the advanced hydraulic piston corer during Leg 149 and is therefore the only hole with good sediment recovery and reliable paleomagnetic data. Most of the sediments consist of clay, nannofossil ooze, nannofossil clay, silty clay and clayey silt, silt, and fine sand. Calcareous nannofossils are well preserved and abundant in most of the samples (Tables 5, 6).

Pleistocene

Samples 149-898A-1H-1, 2-3 cm, to 1H-4, 145-146 cm, are assigned to the *Emiliania huxleyi* Zone (NN21), based on the occurrence of *E. huxleyi*.

Table 4. Distribution of Pliocene calcareous nannofossils, Hole 897C.

Age	Nannofossil zone		Abundance	Preservation	Fossil Species																																		
	Core, section, interval (cm)	Depth (mbsf)			<i>Anaerolithus delicatus</i>	<i>Ceratolithus rugosus</i>	<i>Calcidiscus leptoporus</i>	<i>C. macintyreii</i>	<i>Coccolithus pelagicus</i>	<i>Diacyclops productus</i>	<i>D. perplexa</i>	<i>Discosaster asymmetricus</i>	<i>D. brouweri</i>	<i>D. challengerii</i>	<i>D. intercalaris</i>	<i>D. pentaradiatus</i>	<i>D. surculus</i>	<i>D. tamalis</i>	<i>D. tricubitus</i>	<i>D. variabilis</i>	<i>Geminitithella rotula</i>	<i>Gephyrocapsa caribbeanica</i>	<i>G. sp.</i>	<i>G. spp. (<3 µm)</i>	<i>Helicosphaera acuta</i>	<i>H. carteri</i>	<i>H. sellii</i>	<i>H. wuicchi</i>	<i>Pontosphaera anisotrema</i>	<i>P. discopora</i>	<i>P. japonica</i>	<i>Pseudomilliamia lacunosa</i>	<i>Reiniculofenestra gelida</i>	<i>R. doronicoides</i>	<i>R. minuta</i>	<i>R. minutula</i>	<i>R. pseudoumbilicus</i>	<i>Rhabdosphaera claviger</i>	<i>Syracosphaera pulchra</i>
late Pliocene	NN 19a	14R-4, 88-89	181.18	V	G	.	.	A	F	A	F	A	A	C	F	R	.	F	.	.	.	A	A	.	A	A	.	R	.	.	.	
		15R-1, 127-128	186.67	V	G	.	.	A	F	F	A	F	C	A	F	.	C	R	.	.	F	A	A	.	A	A	r
		15R-2, 115-116	188.05	V	G	.	.	A	C	F	A	F	A	A	F	C	F	.	F	.	A	A	.	C	A	.	F	F	.	.
		16R-2, 113-114	197.73	V	G	.	.	A	A	A	A	F	.	C	C	.	.	.	A	C	.	A	C	.	C	C	.	.	
		16R-3, 112-113	199.22	V	G	.	.	A	C	C	A	F	F	R	F	F	.	C	R	A	C	.	A	C	.	F	.	.	.	
		16R-4, 41-42	200.01	V	G	.	.	A	A	A	C	r	C	C	.	A	C	
		17R-1, 17-18	204.87	V	G	.	.	A	A	C	C	F	.	.	F	.	.	.	C	C	.	A	C	
		17R-2, 80-81	207.17	V	G	.	.	A	C	A	C	F	R	F	F	.	.	.	C	A	.	A	A	.	F	F	.	.	
	NN 18	17R-3, 17-18	207.87	A	G	.	.	C	C	C	C	R	.	R	R	R	F	F	.	R	F	C	C	.	A	C	.	R	.	.	.
		18R-1, 37-38	214.77	V	G	.	.	C	F	F	A	R	.	F	C	F	.	A	F	
		19R-1, 18-19	224.28	V	G	.	.	A	C	C	F	.	.	R	.	.	.	R	F	.	.	.	A	C	.	A	C	r	.	F	.	.	
		19R-1, 70-71	224.80	A	M	.	.	C	F	A	F	F	.	.	.	F	.	.	.	F	.	.	C	F	.	A	F	
		19R-2, 135-136	226.95	A	M	.	.	C	R	C	F	F	F	R	.	.	F	.	.	.	C	F	.	C	F	.	F	.	.	.	
		19R-3, 52-53	227.62	A	P	.	.	C	R	C	C	R	R	C	.	.	r	
		19R-3, 85-86	227.95	B	P
		19R-4, 93-94	229.53	V	G	.	.	C	F	A	A	F	.	F	.	.	R	C	R
		20R-1, 133-134	235.13	V	G	.	.	C	F	C	A	R	C	F	C	F	.	C	F	
		20R-2, 42-43	235.72	V	G	.	.	C	C	C	C	.	R	R	R	.	.	C	F	C	C	C	.	F	C	F	.	C	F	.	F	R	.	.	
		21R-1, 3-4	243.43	V	G	.	.	A	C	C	C	R	.	A	C	C	C	.	R	R	A	F	.	C	F	.	F	C	R	
		21R-1, 123-124	244.63	A	G	.	.	C	C	C	F	F	R	R	R	.	F	R	.	.	C	F	.	C	F	.	F	.	R	.	.
		22R-2, 62-63	255.12	A	G	.	.	A	C	C	C	.	C	.	r	R	C	C	.	A	C	
		22R-3, 66-67	256.66	V	G	.	.	C	C	A	C	R	.	F	.	.	R	F	F	C	R	.	F	C	C	.	A	C	.	F	.	.	.	
		22R-4, 32-33	257.82	V	G	.	.	C	C	A	C	.	F	F	F	.	.	C	A	.	A	A	.	F	.	.	
		22R-4, 106-107	258.56	V	G	.	.	C	C	C	C	.	F	F	F	F	.	R	.	R	A	C	.	A	C	.	R	.	.	
		23R-1, 58-59	263.28	B
	23R-1, 113-114	263.83	V	G	.	.	A	C	A	C	R	.	C	F	A	C	.	A	C		
	NN 17	23R-2, 88-89	265.08	V	G	.	.	C	C	C	F	.	r	F	.	R	.	r	R	F	R	.	.	C	C	.	A	C	.	.	.	
		23R-3, 20-21	265.90	V	M	.	.	A	C	A	F	.	.	C	.	R	r	R	C	F	.	A	F	
		24R-1, 8-9	272.38	A	M	.	.	A	C	C	F	.	.	C	.	R	.	.	R	C	C	.	C	F	
24R-1, 26-27		272.56	V	M	.	.	A	C	A	F	.	.	C	.	.	.	R	R	.	.	C	R	.	A	C		
24R-1, 86-87		273.16	C	M	.	.	C	C	C	C	F	R	F	R	.	R	C	C	.	C	C		
24R-2, 29-30		274.09	A	M	.	.	C	F	C	C	F	r	R	.	.	r	.	.	R	.	.	.	R	R	R	.	.	C	C	.	C	C	.	R	.	.	.		
25R-1, 6-7		282.06	V	G	.	.	A	C	A	F	.	.	.	C	A	R	.	A	A		
25R-1, 90-91		282.90	A	M	.	.	A	R	C	R	.	.	R	.	.	R	.	r	C	C	.	A	C	r		
25R-1, 106-107		283.06	V	G	.	.	A	C	A	F	.	.	R	R	.	F	.	.	A	C	.	C	C	.	A	.	R	.	
25R-2, 19-20		283.69	A	G	.	.	C	C	C	F	.	.	R	F	F	F	R	.	R	C	C	.	A	A	.	R	.	.	
25R-CC, 5-6		284.05	V	M	.	.	A	C	A	.	.	F	C	C	.	A	A		
NN 16		26R-1, 4-5	291.54	V	G	.	.	C	C	C	C	.	r	C	.	.	F	C	C	C	.	F	.	A	F	.	A	A	.	.	
	26R-1, 22-23	291.72	V	G	.	.	C	C	C	.	.	C	.	.	R	R	.	F	F	.	.	.	C	A	.	A	C		
	26R-1, 35-36	291.85	A	G	.	.	C	C	C	F	R	F	.	.	F	R	F	.	.	C	C	.	C	C		
	26R-1, 49-50	291.99	V	M	.	.	C	C	C	C	F	.	C	.	.	F	C	C	F	.	F	R	.	.	C	F	R	.	C	C	.	.	.		
	26R-1, 71-72	292.21	V	G	.	.	C	F	C	C	.	C	C	.	.	C	C	F	.	C	R	.	.	R	.	.	C		
	26R-1, 93-94	292.43	A	P	.	.	C	C	C	.	.	C	C	.	.	F	C	C	F	F	C	.	C	.	C		
early Pliocene	NN 14/15	26R-2, 6-7	293.06	V	G	.	.	A	C	A	.	.	C	C	.	F	C	C	F	F	C	.	A	.	F			
		26R-2, 108-109	294.08	V	G	.	.	R	C	.	C	C	F	C	C	.	.	F	C	C	.	C	.	F	.	F	R	.	.	F	.	C	.	A	.	C	.		
	?	27R-1, 1-2	301.21	V	M	C	.	C	F	R	.	.	C	A	.	F	C	F	F	F	C	.	.	A			
27R-1, 5-6	301.25	A	M	C	.	C	.	R	.	.	C	F	.	.	C	.	R	F	C	.	.	F				

Note: V = very abundant; A = abundant; C = common; F = few; R = rare; G = good; M = moderate; P = poor; B = barren; r = rare (reworked).

Table 6. Distribution of Pliocene calcareous nannofossils, Hole 898A.

Age	Nannofossil zone	Hole 898A		Abundance	Preservation	<i>Calcidiscus leptoporus</i>	<i>C. macintyreii</i>	<i>Coccolithus pelagicus</i>	<i>Dicryococites productus</i>	<i>D. perplexa</i>	<i>D. pentaradiatus</i>	<i>D. tamalis</i>	<i>D. triradiatus</i>	<i>Geminitella rotula</i>	<i>Gephyrocapsa caribbeanica</i>	G. sp.	G. spp. (<3 µm)	<i>Helicosphaera acuta</i>	<i>H. carteri</i>	<i>H. sellii</i>	<i>Pontosphaera antisotrema</i>	<i>P. discopora</i>	<i>P. japonica</i>	<i>Pseudoemiliana lacunosa</i>	<i>Reticulofenestra doronicoides</i>	<i>R. minuta</i>	<i>R. minutula</i>	<i>Rhabdosphaera claviger</i>	<i>Syracosphaera pulchra</i>	<i>Scapholithus fossilis</i>	<i>Umbilicosphaera sibogae foliosa</i>	<i>Thoracosphaera</i> sp.	
		Core, section, interval (cm)	Depth (mbsf)																														
late Pliocene	NN 19a	16X-4, 103-104	144.33	V	G	A	F	R	A	R	F	C	A	C	C	C	.	F	F	A	C	F	A	.	F	.	.	.	
		16X-5, 42-43	145.22	V	M	A	F	F	C	F	C	C	F	F	F	.	.	R	A	F	C	A	.	F	.	.	.
		17X-1, 12-13	148.62	A	G	A	F	C	C	R	C	C	.	F	C	.	R	.	A	C	C	A	F	.	.	R	.
		17X-1, 88-89	149.38	V	G	A	C	A	F	.	r	C	F	F	F	.	.	.	A	R	A	A
		17X-2, 35-36	150.35	V	G	A	F	A	C	F	r	F	.	F	F	.	.	.	A	F	A	A	.	.	R	.	.
		17X-2, 133-134	151.33	V	G	A	F	C	A	.	r	F	A	F	C	A
		17X-3, 9-10	151.59	V	G	A	F	A	A	R	F	F	F	F	R	F	R	A	R	A	A	F	F	.	.	.
		17X-3, 130-131	152.8	V	G	A	F	C	C	F	F	F	F	C	.	F	.	A	.	A	A	F	F	.	.	.
		17X-4, 106-107	154.06	V	M	A	F	C	C	F	F	.	A	A	.	.	.	A	R	A	A
		17X-5, 23-24	154.73	V	G	A	F	C	.	.	.	r	F	F	A	C	.	F	.	A	.	A	A	.	F	.	R	.
		17X-6, 90-91	156.9	A	G	A	F	C	C	F	C	F	C	.	.	.	A	F	C	A
		17X-CC, 1-2	157.51	V	G	C	F	C	F	F	C	C	C	.	.	F	A	F	C	A	F	F	R	.	.
		18X-1, 42-43	158.52	V	G	A	F	C	C	C	F	C	C	.	F	F	A	.	C	A	C	C	.	R	.
		18X-1, 146-147	159.56	V	G	F	F	F	F	R	.	C	.	.	F	A	.	A	A	F	F	.	.	.
		18X-2, 71-72	160.31	V	G	C	F	F	.	.	.	r	F	F	.	.	.	A	.	A	A	.	F	.	.	.
		18X-2, 91-92	160.51	V	G	C	F	F	R	F	F	.	F	.	A	R	C	A	F	F	R	.	.
		18X-3, 56-57	161.66	V	G	C	R	F	F	F	.	.	.	A	.	F	A
		18X-4, 58-59	163.18	V	G	C	F	F	C	F	F	.	.	C	C	C	C

Note: V = very abundant; A = abundant; C = common; F = few; R = rare; G = good; M = moderate; P = poor; r = rare (reworked)

- FO of *Reticulofenestra asanoi* (>6.5 µm): Sample 149-898A-7H-3, 7-8 cm.
- LO of large *Gephyrocapsa* (>5.5 µm), which corresponds to the LO of *Gephyrocapsa* sp. A-B of Matsuoka and Okada (1990): Sample 149-898A-11H-1, 105-106 cm.
- LO of *Helicosphaera sellii*: Sample 149-898A-11H-1, 105-106 cm.
- FO of large *Gephyrocapsa* (>5.5 µm): Sample 149-898A-14H-4, 30-31 cm.
- LO of *Calcidiscus macintyreii*: Sample 149-898A-16X-2, 100-101 cm.
- FO of *Gephyrocapsa oceanica* s.l. (>4 µm): Sample 149-898A-16X-3, 52-53 cm.

Pliocene

All of the lower Pliocene and most of the upper Pliocene are missing in this hole. Samples 149-898A-16X-4, 103-104 cm, to 18X-4, 58-59 cm, are placed in Zone NN19a, based on the absence of both *Gephyrocapsa oceanica* s.l. (>4µm) and *Discoaster brouweri*. Rare to common *Calcidiscus macintyreii* were observed in this interval along with few to abundant small *Gephyrocapsa*, rare to common *Helicosphaera acuta*, and few to abundant *Helicosphaera carteri* and *Helicosphaera sellii*; rare to few *Gephyrocapsa caribbeanica* occur in the uppermost part of this interval. Reworked *Discoaster pentaradiatus*, *Discoaster tamalis*, and *Discoaster triradiatus* were also recorded. The taxa are abundant to very abundant with moderate to good preservation.

Hole 899A

Hole 899A (40°46.332'N, 12° 12.156'E, at a water depth of 5291.0 m) was drilled to 81.5 m below seafloor (mbsf) before a core was tak-

en; therefore, all of the Pleistocene sediments were washed away. The first core was recovered from the Pliocene.

Samples 149-899A-1R-1, 23-24 cm, to 1R-2, 19-20 cm, contain neither *Gephyrocapsa oceanica* s.l. (>4 µm) nor *Discoaster brouweri*; hence, they are assigned to the upper Pliocene Zone NN19a. These samples also contain common *Calcidiscus macintyreii*, abundant *Pseudoemiliana lacunosa* and *Reticulofenestra minutula*, and few *Helicosphaera acuta*. Nannofossils are very abundant and have good preservation in this zone.

NN18 (*Discoaster brouweri* Zone) is recognized from Samples 149-899A-1R-3, 135-136 cm, to 4R-1, 40-41 cm. The relative abundance of *Discoaster brouweri* is few to rare in this interval. *Discoaster triradiatus* occurs in the uppermost part of the zone. Nannofossils are abundant to very abundant and exhibit moderate to good preservation.

The LO of *Discoaster pentaradiatus* occurs between Samples 149-899A-4R-1, 40-41 cm, and 4R-1, 61-62 cm, and marks the top of Zone NN17 (*Discoaster pentaradiatus* Zone), which is represented by a very short interval. In this zone, the lowest occurrence of *Helicosphaera acuta* is present. Samples 149-899A-4R-2, 79-80 cm, to 6R-1, 86-87 cm, are placed in NN16 (*Discoaster surculus* Zone); *Discoaster pentaradiatus* and *D. surculus* are both present in this interval. The highest occurrences of *D. asymmetricus* (Sample 149-899A-4R, CC) and *Discoaster tamalis* (Sample 149-899A-5R-1, 72-73 cm) were also noted within the zone. The overall assemblage consists mainly of abundant to common *Calcidiscus leptoporus*, *Coccolithus pelagicus*, and *Pseudoemiliana lacunosa*; rare to common *Calcidiscus macintyreii*; and common *Discoaster brouweri*. Nannofossils are common to very abundant with moderate to good preservation.

Zone NN14 (*Discoaster asymmetricus* Zone) and Zone NN15 (*Reticulofenestra pseudoumbilicus* Zone) were combined in this

Table 7. Distribution of Pliocene calcareous nannofossils, Hole 899A.

Age	Nannofossil zone	Hole 899A Core, section, interval (cm)	Depth (mbsf)	Abundance	Preservation	<i>Amaurolithus delicatus</i>	<i>A. tricorniculatus</i>	<i>Calcidiscus leptoporus</i>	<i>C. macintyreii</i>	<i>Ceratiolithus cristatus</i>	<i>Coccolithus pelagicus</i>	<i>Dicoyococites productus</i>	<i>D. perplexa</i>	<i>Discoaster asymmetricus</i>	<i>D. brouweri</i>	<i>D. challengeri</i>	<i>D. intercalaris</i>	<i>D. pentaradiatus</i>	<i>D. surculus</i>	<i>D. tamalis</i>	<i>D. triradiatus</i>	<i>D. variabilis</i>	<i>Geminitithella rotula</i>	<i>Gephyrocapsa caribbeanica</i>	<i>Gephyrocapsa</i> sp.	<i>G. spp. (<3 μm)</i>	<i>Helicosphaera acuta</i>	<i>H. carteri</i>	<i>H. sellii</i>	<i>H. waltichi</i>	<i>Oolithon fragile</i>	<i>Pontosphaera anisostrema</i>	<i>P. discopora</i>	<i>P. japonica</i>	<i>Pseudoemiliania lacunosa</i>	<i>Reticulofenestra darwinoides</i>	<i>R. gelida</i>	<i>R. minuta</i>	<i>R. minutula</i>	<i>R. pseudoubilicus</i>	<i>Rhabdosphaera claviger</i>	<i>Sphenolithus</i> spp.	<i>Syracosphaera pulchra</i>	<i>Thoracosphaera</i> sp.			
late Pliocene	NN 19a	1R-1, 23-24	81.73	V	G	.	.	C	C	F	F	F	F	A	A	R	A	A	.	.	.	R						
		1R-2, 19-20	83.19	V	G	.	.	F	C	.	C	A	R	F	F	F	R	.	.	.	R	R	A	A	C	C			
	NN 18	1R-3, 135-136	85.85	A	G	.	.	F	C	.	C	A	.	R	F	.	R	.	R	C	F	C	R	.	.	.	F	A	A	R	A	A	C	F		
		1R-CC	86.00	A	G	.	.	C	C	.	F	F	.	R	F	.	R	.	C	.	C	.	.	.	F	C	C	C	C	r	F				
		2R-1, 43-44	91.53	A	G	.	.	C	C	.	C	C	.	r	F	R	.	R	C	F	.	C	.	.	.	R	C	C	C	C	C	F				
		2R-2, 52-53	93.12	A	G	.	.	C	C	.	C	C	F	r	F	F	.	C	.	C	C	C	.	R	.	C	C	C	R	C	C	F			
		3R-3, 109-110	104.89	V	M	.	.	C	C	.	C	F	.	F	C	C	C	C	R				
		3R-CC	105.30	V	M	.	.	C	C	.	C	F	R	R	R	R	C	C	.	F	C	.	.	.	R				
		4R-1, 40-41	110.8	V	G	.	.	C	C	.	C	F	.	.	F	F	C	C	F	C	C	C		
	NN 17	4R-1, 61-62	111.01	V	G	.	.	C	C	.	C	C	F	F	F	F	.	.	.	F	.	C	C	.	A	A			
		4R-2, 79-80	112.69	V	G	.	.	A	F	.	C	C	.	F	.	.	C	R	C	C	.	A	C		
	NN 16	4R-2, 114-115	113.04	C	G	.	.	C	C	R	A	F	.	C	.	.	C	F	R	F	C	C	.	A	C	
		4R-CC	113.40	V	M	.	.	C	C	.	C	R	.	F	C	C	F	C	C	
		5R-1, 72-73	120.80	V	M	.	.	A	C	R	C	R	.	F	C	.	.	.	F	C	R	C	F	.	A	A	
		5R-1, 116-117	121.26	V	G	.	.	C	C	.	C	R	.	F	C	.	.	.	F	F	F	R	.	.	R	C	F	.	A	C	
		5R-2, 6-7	121.66	V	G	.	.	A	C	.	A	F	.	F	C	C	F	C	R	C	C	
		5R-2, 44-45	122.04	V	M	.	.	A	F	.	C	C	R	F	C	.	.	.	R	F	F	F	C	F	.	A	C	
		5R-2, 99-100	122.59	A	G	.	.	A	F	.	A	C	C	.	C	.	.	.	F	R	.	.	F	R	.	R	.	.	R	.	.	.	A	F	.	A	A	r	R				
		5R-3, 17-18	131.27	V	G	.	.	C	R	.	C	C	F	.	C	.	.	.	F	R	F	R	.	R	.	C	C	.	A	C	
		5R-3, 49-50	131.59	V	G	.	.	C	F	.	A	C	C	.	C	C	A	F	.	A	A	
		5R-CC	129.70	A	M	.	.	C	F	.	C	C	F	F	C	C	F	F	.	R	C	.	R	A	C
		6R-1, 7-8	129.77	V	G	.	.	A	C	.	A	.	.	.	C	C	A	F	R	C	.	A	A
		6R-1, 86-87	130.56	V	G	.	.	C	F	.	C	F	C	C	.	.	.	R	C	C	F	R	F	C	A	.	A	A
	early Pliocene	NN 14/15	6R-2, 104-105	132.24	V	M	C	.	C	F	.	C	C	F	C	.	.	F	C	C	F	.	C	.	C	F	.	F	C	.	.	.	A	.	F	A	A	C
			6R-3, 2-3	132.72	V	M	C	.	C	F	.	C	C	C	C	.	.	.	C	C	F	C	.	C	.	F	.	.	F	F	.	.	.	C	.	F	A	A	C
6R-3, 97-98			133.67	V	M	C	.	C	F	.	C	C	C	F	C	.	.	.	F	C	F	F	.	F	.	.	.	F	R	.	.	.	F	.	C	C	C
6R-4, 40-41			175.10	V	M	C	.	C	F	.	C	C	C	.	F	.	.	.	C	C	F	F	.	C	A	C
6R-CC			139.00	V	M	C	.	C	F	.	C	F	F	C	C	.	.	.	F	C	C	F	.	R	F	R	.	.	.	F	.	C	A	C	C
7R-1, 40-41		139.4	V	M	C	.	A	F	.	F	F	A	.	C	.	R	F	A	C	.	R	R	F	.	.	.	R	C	C	C	
?		7R-1, 81-82	139.81	V	M	C	R	A	R	.	F	F	A	.	F	.	.	A	F	.	R	C	A	C	C	F			
	7R-CC	148.7	A	G	C	.	C	.	.	R	F	C	.	F	.	.	R	C	C	C	C	F		

Note: V = very abundant; A = abundant; C = common; F = few; R = rare; G = good; M = moderate; P = poor; r = rare (reworked).

hole, because the LO of *Amaurolithus tricorniculatus* was not found. The LO of *Reticulofenestra pseudoubilicus* marks the top of this NN14-15 interval; the base is defined by the FO of *Pseudoemiliania lacunosa*. The highest occurrence of *Amaurolithus delicatus* is recognized at the top of Zone NN14-15. The co-occurrences of *Helicosphaera sellii* and *Discoaster tamalis* may suggest an unconformity at the base of Core 149-899A-6R. Nannofossils are very abundant with moderate preservation in this interval.

Samples 149-899A-7R-1, 40-41 cm, to 7R-CC, are assigned to the lower Pliocene. This interval is characterized by common *Amaurolithus delicatus*, rare *Amaurolithus tricorniculatus*, few to common *Discoaster brouweri* and *Discoaster surculus*, abundant to rare *Discoaster pentaradiatus*, rare *Discoaster triradiatus*, and common *Reticulofenestra pseudoubilicus* and *Reticulofenestra gelida*. Nannofossils are abundant to very abundant with moderate to good preservation in this zone.

Hole 900A

Pliocene-Pleistocene sediments recovered in the top 11 cores of Hole 900A (46°40.992'N, 11°36.252'E, at a water depth of 5036.8 m) consist mainly of nannofossil ooze, nannofossil clay, nannofossil chalk, nannofossil claystone, clay, claystone, silt, and fine sand. Calcareous nannofossils are well preserved and abundant in most of the samples (Tables 8, 9).

Pleistocene

Samples 149-900A- 1R-1, 24-25 cm, to 2R-CC are assigned to the *Gephyrocapsa oceanica* Zone (NN20), based on the absence of both *Emiliania huxleyi* and *Pseudoemiliania lacunosa*.

Samples 149-900A-3R-1, 8-9 cm, to 6R-2, 110-111 cm, are assigned to *Pseudoemiliania lacunosa* Zone (NN19), based on the occurrence of *Pseudoemiliania lacunosa* and *Gephyrocapsa oceanica* s.l. (>4μm). The additional events used to further subdivide the *Pseudoemiliania lacunosa* Zone are recognized as the following:

1. LO of *Reticulofenestra asanoi* (>6.5 μm): Sample 149-900A-4R-1, 19-20 cm.
2. Reoccurrence of *Gephyrocapsa oceanica* (>3 μm), which corresponds to the FO of *Gephyrocapsa* sp. C-D of Matsuoka and Okada (1990): Sample 149-900A-4R-1, 46-47 cm.
3. FO of *Reticulofenestra asanoi* (>6.5 μm): Sample 149-900A-4R-4, 132-133 cm.
4. LO of large *Gephyrocapsa* (>5.5 μm), or LO of *Gephyrocapsa* sp. A-B (Matsuoka and Okada, 1990): Sample 149-900A-5R-1, 74-75 cm.
5. LO of *Helicosphaera sellii*: Sample 149-900A-5R-1, 74-75 cm.
6. FO of large *Gephyrocapsa* (>5.5 μm): 149-900A-5R-3, 37-38 cm.

Table 8. Distribution of Pleistocene calcareous nannofossils, Hole 900A.

Age	Nannofossil zone	Hole 900A		Abundance	Preservation	Fossil Species																														
		Core, section, interval (cm)	Depth (mbsf)			<i>Calcidiscus leptoporus</i>	<i>C. macintyreii</i>	<i>Ceratolithus cristatus</i>	<i>Coccolithus crassispinus</i>	<i>C. pelagicus</i>	<i>Dicycococites perplexa</i>	<i>D. productus</i>	<i>Discoaster</i> spp. (reworked)	<i>Gephyrocapsa caribbeanica</i> (3–4 µm)	<i>G. caribbeanica</i> (4–5.5 µm)	<i>G. caribbeanica</i> (>5.5 µm)	<i>G. oceanica</i> (3–4 µm)	<i>G. oceanica</i> (4–5.5 µm)	<i>G. oceanica</i> (>5.5 µm)	<i>G. spp.</i> (<3 µm)	<i>Helicosphaera carteri</i>	<i>H. sellii</i>	<i>Pontosphaera discopora</i>	<i>P. japonica</i>	<i>Pseudoemiliana lacunosa</i> (elliptical)	<i>P. lacunosa</i> (round)	<i>Reticulofenestra asanovi</i> (>6 µm)	<i>R. minuta</i> (<3 µm)	<i>R. minutula</i> (3–5 µm)	<i>R. sp. A</i> (5–6 µm)	<i>Rhabdosphaera clavigera</i>	<i>Scapholithus fossilis</i>	<i>Syracosphaera pulchra</i>	<i>Thorasphaera</i> spp.	<i>Umbilicosphaera sibogae</i>	
Pleistocene	NN20	1R-1, 22–23	0.22	V	G	A	.	.	F	F	R	R	.	.	F	C	C	.	V	C	V	C	.	C	F	C	R	C			
		1R-2, 28–29	1.08	V	G	A	.	.	R	R	R	R	F	.	.	.	F	C	.	A	C	V	C	.	C	R	R	R	C		
		1R-CC	1.50	A	G	A	.	.	R	R	R	R	F	C	.	A	C	.	R	R	.	.	V	C	.	C	F	C	R	C		
		2R-1, 6–7	1.56	V	G	A	.	.	C	F	R	R	F	F	.	A	C	.	R	.	.	.	V	C	.	C	R	F	R	F		
		2R-1, 30–31	1.80	V	G	A	.	.	C	F	F	V	.	C	.	.	A	F	.	A	F	A	A	.	F	.	F	R	F		
		2R-1, 42–43	1.92	V	G	A	.	.	C	F	R	V	.	C	.	.	A	F	.	A	C	V	A	.	F	.	F	R	F		
		2R-CC	10.10	V	G	C	.	.	R	.	.	V	.	C	.	.	A	F	.	V	F	V	A	.	F	.	.	R	F		
		3R-1, 8–9	10.18	V	G	C	.	R	F	R	.	V	.	C	.	.	A	F	.	A	C	A	F	.	A	A	.	C	.	R	F
	3R-1, 21–22	10.31	V	G	A	.	.	R	.	.	R	A	A	F	.	A	C	A	F	.	V	A	.	C	.	R	C	
	3R-1, 85–86	10.95	V	G	A	R	V	C	F	.	V	R	.	F	.	.	A	F	.	V	F	.	R	F	F	R	F
	3R-1, 135–136	11.45	V	G	A	.	.	R	R	.	V	C	F	.	V	F	.	R	.	.	A	F	.	V	F	.	R	R	F	R	F
	3R-2, 7–8	11.67	V	G	A	.	.	R	.	.	A	C	F	.	A	C	.	R	.	.	A	F	.	V	A	F	
	3R-2, 20–21	11.80	V	G	A	.	.	R	.	.	A	C	F	.	V	F	.	R	.	.	A	F	.	C	F	R	F	F	F	R	F
	4R-1, 4–5	20.84	V	G	A	.	.	R	R	R	V	.	F	.	.	.	C	F	.	V	F	A	C	.	A	F	R	F	F	F	R	F
	4R-1, 19–20	20.99	V	G	A	.	.	R	R	.	R	.	C	.	.	.	A	C	.	V	C	.	F	.	.	V	C	C	V	C	F	F	F	A	R	R
	4R-1, 46–47	21.26	V	G	A	.	.	R	C	.	.	.	A	C	.	V	C	.	R	.	.	A	C	A	V	C	F	C	.	R	R	C
	4R-1, 96–97	21.76	V	G	A	.	.	R	A	F	V	C	A	V	C	F	F	R	F	R	C
	4R-1, 129–130	22.09	V	G	A	.	.	R	R	A	.	F	R	A	F	A	V	C	F	F	R	F	R	F		
	4R-2, 16–17	22.46	V	G	A	.	.	R	.	.	F	V	F	.	R	.	.	A	F	A	V	C	F	F	.	F	R	F
	4R-2, 110–111	23.40	V	G	A	V	C	.	F	.	.	A	C	V	C	C	R	F	R	F		
	4R-3, 50–51	24.30	V	G	A	A	C	.	F	.	.	A	C	C	V	C	C	F	.	F	R	F
	4R-3, 84–85	24.64	V	G	A	.	.	R	A	C	.	F	.	.	A	C	A	V	C	A	F	.	F	R	F
	4R-3, 122–123	25.02	V	G	A	A	F	.	R	R	A	C	C	V	F	A	F	.	F	R	F	
	4R-4, 77–78	26.07	V	G	A	.	.	R	F	A	F	.	R	.	.	A	F	C	V	F	C	F	R	F	R	
	4R-4, 132–133	26.62	V	G	A	.	.	F	.	.	R	A	F	.	F	R	A	C	C	A	C	C	F	.	F	R	F	
	4R-5, 80–81	27.60	V	G	A	.	.	R	F	.	F	A	F	.	R	.	.	A	F	.	A	F	C	F	R	F	R	F
	4R-CC	30.40	V	G	A	.	.	R	A	C	.	R	R	V	C	.	V	C	A	F	.	F	R	C	
	5R-1, 74–75	31.14	V	G	A	.	.	F	F	A	F	r	.	C	F	.	C	F	V	F	F	R	A	C	.	A	F	.	C	R	F	R	.			
	5R-1, 114–115	31.54	V	G	A	.	.	F	C	A	C	.	F	A	F	.	A	F	A	F	F	F	.	A	C	.	A	C	.	F	.	F	R	F		
	5R-2, 19–20	32.09	V	G	A	.	.	F	F	A	A	.	F	A	F	.	A	F	V	F	F	F	.	A	F	.	A	C	.	F	F	F	R	R		
	5R-2, 93–94	32.83	V	G	A	.	.	F	C	C	C	.	F	A	V	C	C	A	R	R	C	F	.	A	C	.	F	.	F	R	R	
	5R-3, 37–38	33.77	V	G	C	.	.	F	F	F	F	.	F	A	V	C	A	C	C	F	R	R	.	A	F	.	A	A	.	F	R	F	R	R		
	5R-4, 80–81	35.70	V	G	A	.	.	F	C	C	C	.	C	A	.	A	C	.	C	R	R	R	.	C	F	.	A	C	.	F	.	F	R	R		
	5R-5, 72–73	37.12	V	G	A	.	.	C	F	C	V	.	C	A	.	C	A	.	C	F	F	R	.	C	R	.	A	A	.	R	.	R	R			
	5R-CC	40.00	V	G	F	.	.	R	R	.	F	.	F	F	.	F	F	.	F	R	R	R	.	R	R	.	R	R	.	R	.	R	R			
	6R-1, 12–13	40.12	V	G	C	.	.	C	C	.	A	.	C	A	.	C	A	.	C	F	F	.	.	.	A	C	.	A	A	.	R	.	F	R	R	
	6R-2, 30–31	41.80	V	G	A	.	.	C	C	.	A	.	C	F	.	C	C	.	C	F	F	.	.	.	C	F	.	A	V	.	R	.	R	R		
	19b	6R-2, 110–111	43.20	V	G	A	R	.	F	C	.	A	.	F	.	.	C	.	.	A	F	F	R	R	A	F	.	A	A	.	F	.	F	R	.	

Note: V = very abundant; A = abundant; C = common; F = few; R = rare; G = good; M = moderate; P = poor; r = rare (reworked).

- LO of *Calcidiscus macintyreii*: Sample 149-900A-6R-2, 30-31 cm.
- FO of *Gephyrocapsa oceanica* s.l. (>4 µm): Sample 149-900A-6R-2, 110-111

Pliocene

The uppermost Pliocene Zone NN19a is assigned from Samples 149-900A-6R-3, 86-87 cm, to 6R-5, 136 cm, where neither *Gephyrocapsa oceanica* s.l. (>4 µm) nor *Discoaster brouweri* is present. This interval is characterized by abundant to rare small *Gephyrocapsa*, common *Gephyrocapsa caribbeanica* in the upper part of the zone, and few to common *Calcidiscus macintyreii*, *Helicosphaera acuta*, and *Helicosphaera sellii*.

Zone NN18 (*Discoaster brouweri* Zone) is recognized from Samples 149-900A-6R-6, 78-79 cm, to 8R-CC, where *Discoaster brouweri* is present. *Discoaster triradiatus* is present in the upper part of this zone, as is *Helicosphaera acuta*. Nannofossils are common to very abundant with moderate to good preservation.

Samples 149-900A-9R-1, 45-46 cm, to 10R-4, 69-70 cm, are assigned to the Zone NN16 (*Discoaster surculus* Zone). The highest occurrences of *Discoaster pentaradiatus* and *Discoaster surculus* were found in the same sample, and Zone NN17 is missing in this hole. The main assemblage in this zone is characterized by rare to common *Discoaster brouweri*, *Discoaster pentaradiatus*, and *Discoaster surculus*; rare *Discoaster triradiatus*; few to rare and sporadic *Helicosphaera sellii*; and few to abundant *Pseudoemiliana lacunosa*. The highest occurrences of both *Discoaster asymmetricus* and *Discoaster tamalis* were recorded within this zone in the same sample. Nannofossils are abundant to very abundant and exhibit good preservation.

Samples 149-900A-11R-1,72-73 cm, to 11R-4, 119-120 cm, are assigned to the combined Zones NN14 and NN15 (*Discoaster asymmetricus* Zone/*Reticulofenestra pseudumbilicus* Zone) according to the presence of *Pseudoemiliana lacunosa* and *Reticulofenestra pseudumbilicus*. *Discoaster asymmetricus* is not present at the base of this interval. The LO of *Amaurolithus delicatus* is recorded within this interval, as is the FO of *Discoaster tamalis*. Nannofossils are

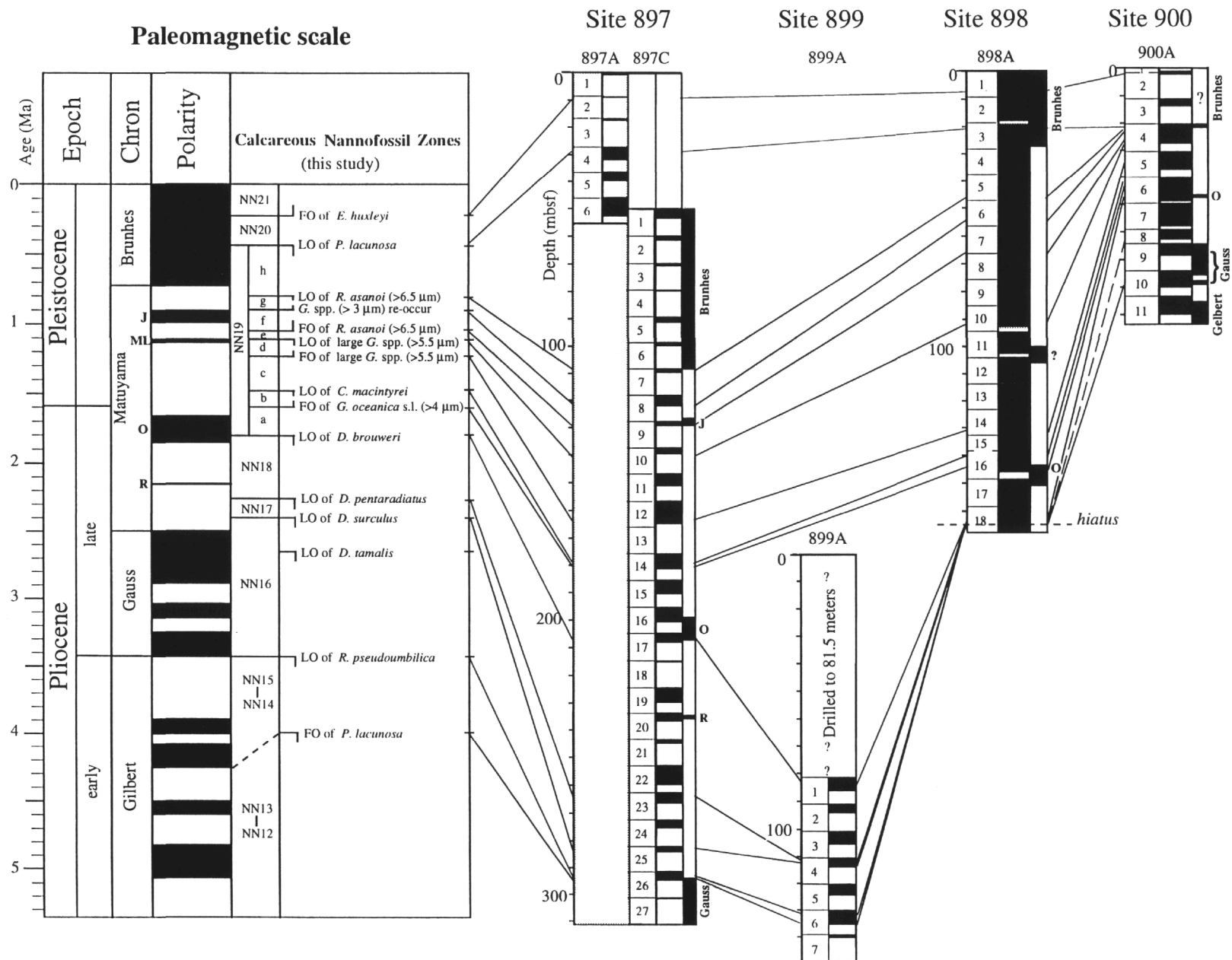


Figure 2. Correlation of Pliocene-Pleistocene nannofossil biostratigraphy with magnetostratigraphy at Leg 149 Sites 897, 898, 899, and 900. The paleomagnetic polarity is shown on the right side, core recovery in the middle, and core number on the left for each site.

(0.99-1.07 Ma). However, nannofossil biostratigraphic data indicate that the sediments between 95.75 and 128.00 mbsf belong to NN19d because of the presence of large *Gephyrocapsa* (>5.5 μm). Thus, the age of the second normal polarity interval may correspond to the Cobb Mountain subchron (1.1-1.3 Ma), which occurs earlier than the Jaramillo subchron (0.99-1.07 Ma).

Based on the nannofossil biostratigraphy of Hole 898A, the Jaramillo subchron should be located in NN19f (54.69 to 66.00 mbsf), between the FO of *R. asanoi* (>6.5 μm) and the reoccurrence of *Gephyrocapsa* spp. (>3 μm) events (Fig. 2). However, no paleomagnetic normal signal was identified in that interval. It is obvious that the paleomagnetic data and nannofossil biostratigraphy do not combine well to identify the Jaramillo subchron. Because the resolution and reliability of the nannofossil biostratigraphy in Hole 898A is high enough to clearly identify NN19f and NN19d, there is no reason to assign the second normal polarity interval to the Jaramillo subchron based on nannofossil biostratigraphy.

If we consider the second normal polarity interval as the Cobb Mountain subchron, a possible explanation as to why we discerned the shorter Cobb Mountain subchron without identifying the longer Jaramillo subchron is that the sediment-accumulation rate within NN19d, which includes the Cobb Mountain subchron, is much higher than within NN19f, which includes the Jaramillo subchron (Fig. 2). Another possible explanation is that the Cobb Mountain subchron was recorded by the high-resolution U-channel sample with a sampling interval of only 0.02 m, which makes it much less likely to be ignored than the Jaramillo subchron, which could have been represented by four or five samples within a sampling interval of 5 to 10m.

The third normal polarity interval (143.85 to 161.82 mbsf) lies immediately below the Pliocene/Pleistocene boundary (i.e., the FO of *G. oceanica* s.l.). Therefore, this interval corresponds to the Olduvai subchron based on nannofossil biostratigraphy.

Site 900

Five normal polarity intervals were identified in Hole 900A. From top to bottom, the first normal polarity interval (0.00 to 21.08 mbsf) lies right above the LO of *R. asanoi* (>6.5 μm) and is thus identified as the Brunhes chron (0-0.78 Ma). The second normal polarity interval (47.00 to 48.15 mbsf) was found around the NN18/NN19 boundary (LO of *D. brouweri*), which coincides with the Olduvai subchron (1.65-1.88 Ma). According to nannofossil biostratigraphy, the Jaramillo subchron (0.99-1.07 Ma) should be located in NN19f (21.76 to 26.62 mbsf). However, no sample from this interval was analyzed by paleomagnetic techniques, and thus the Jaramillo subchron was not identified. The third and fourth normal polarity intervals (64.55 to 76.9 mbsf and 78.67 to 79.19 mbsf) are found in NN16; these coincide with the Gauss chron. The upper boundary of the third normal polarity interval represents the Matuyama/Gauss boundary at 2.45 Ma. The lower boundary of the fourth normal polarity interval coincides with the Gauss/Gilbert boundary (3.41 Ma). The fifth normal polarity interval (86.18 to 89.39 mbsf) lies in NN14/15, which probably indicates the uppermost subchron (Cochiti subchron) of the Gilbert chron. From the above data, we see a good correlation between the nannofossil and paleomagnetic analytical results.

Sediment-accumulation Rates Inferred by Nannofossil Biostratigraphy

Figure 3 shows sediment-accumulation rates calculated by assigning each discerned nannofossil event an absolute age based on past studies (Martini and Müller, 1986; Sato and Takayama, 1992; Wei, 1993) as shown below:

FO of <i>Emiliania huxleyi</i>	0.24 Ma
LO of <i>Pseudoemiliania lacunosa</i>	0.39 Ma
LO of <i>Reticulofenestra asanoi</i>	0.83 Ma

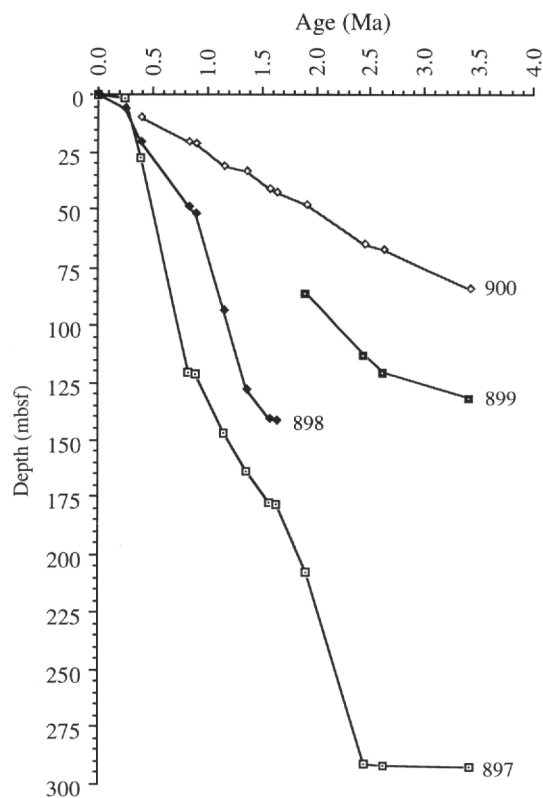


Figure 3. Sedimentation rates at Sites 897, 898, 899, and 900 inferred from the nannofossil biostratigraphy.

Reoccurrence of <i>Gephyrocapsa</i> spp. (>3 μm)	0.89 Ma
LO of <i>Gephyrocapsa</i> spp. (>5.5 μm)	1.15 Ma
FO of <i>Gephyrocapsa</i> spp. (>5.5 μm)	1.36 Ma
LO of <i>Calcidiscus macintyreii</i>	1.57 Ma
FO of <i>Gephyrocapsa</i> s.l. (>4 μm)	1.64 Ma
LO of <i>Discoaster brouweri</i>	1.91 Ma
LO of <i>Discoaster surculus</i>	2.45 Ma
LO of <i>Discoaster tamalis</i>	2.63 Ma
LO of <i>Reticulofenestra pseudumbilicus</i>	3.41 Ma

As shown in Figure 3, the order of the Pliocene-Pleistocene sedimentation rates from highest to lowest at the four Leg 149 sites is Sites 897, 898, 899, and 900. The water depths of these four sites are 5320.0, 5279.0, 5291.0, and 5036.8 m. The general trend of sedimentation rates for Leg 149 indicates that the sedimentation rate increases from the continental margin to the deep sea along with the increasing water depth.

CONCLUSIONS

The Pliocene-Pleistocene calcareous nannofossils of Leg 149 are abundant and well preserved in most of the samples examined. Holes 897C and 898A yielded significant Pliocene-Pleistocene sediments, which provided a high-resolution nannofossil biostratigraphy essential for locating paleomagnetic polarity events and interpreting the age and frequency of turbidite sedimentation in the Iberia Abyssal Plain (as discussed by Zhao et al., this volume, and Milkert et al., this volume).

The Pleistocene nannofossil zonal scheme in this paper is a modification of the schemes proposed by Gartner (1977), Pujos (1985), Takayama and Sato (1987), Matsuoka and Okada (1989, 1990), Sato

and Takayama (1992), and Wei (1993). The Pliocene/Pleistocene boundary was defined by the FO of *Gephyrocapsa oceanica* s.l. (>4 µm). The LO of *Helicosphaera sellii* and the LO of large *Gephyrocapsa* cannot be clearly distinguished in the Leg 149 sediments. The FO of *Emiliania huxleyi*, LO of *Pseudoemiliania lacunosa*, LO of *Reticulofenestra asanoi*, reoccurrence of *Gephyrocapsa oceanica* (>3 µm), and FO and LO of large *Gephyrocapsa* (>5.5 µm) are useful and reliable Pliocene-Pleistocene nannofossil events for subdividing Zone NN19 and thus improve considerably the resolution of the Pleistocene nannofossil biostratigraphy.

The standard zonation of Martini (1971) was followed in this study for the Pliocene biostratigraphy; the definition of Zone MNN19a by Rio et al. (1990a) was followed in the uppermost Pliocene. In the lower Pliocene Zones NN14 and NN15 were combined, as suggested by Raffi and Rio (1979) and Rio et al. (1990b); but the FO of *Discoaster asymmetricus* was replaced by the FO of *Pseudoemiliania lacunosa*. The lowermost Pliocene was not always recorded at these sites, and an unconformity may be suggested between the Miocene and the lower Pliocene sediments in Holes 897C, 899A, and 900A; a more evident break in the sedimentary record occurs in Hole 898A, where all the lower Pliocene and part of upper Pliocene are absent.

Pliocene-Pleistocene nannofossil events reveal that the sedimentation rates along the transition from the Iberian Peninsula to Iberia Abyssal Plain increase from the continental margin to the deep sea along with increasing of water depth.

Pliocene-Pleistocene nannofossil biostratigraphic results for Holes 897C and 900A coincide rather well with the magnetostratigraphy. The combination of nannofossil biostratigraphic and paleomagnetic studies can provide important information for fulfilling the second objective of this leg: to determine the history of turbidite sedimentation in the Iberia Abyssal Plain.

REMARKS ON PROBLEMATIC SPECIES

Genus GEPHYROCAPSA Kamptner, 1943

Gephyrocapsa caribbeanica Boudreaux and Hay, 1969

Remarks. Specimens of *Gephyrocapsa* 3.0-5.5 µm in size and with a small central area are included under this species name. The lowest occurrence of *Gephyrocapsa caribbeanica* was generally recorded from Zone NN19a except for Hole 899A.

Small *Gephyrocapsa* spp.

Remarks. Very small specimens of *Gephyrocapsa* (less than 3 µm in size) are included under this denomination. They were recorded in the lower Pliocene (Zone NN14/15) and in the upper Pliocene (Zone NN18) through the Pleistocene.

Gephyrocapsa sp.

Remarks. Specimens of *Gephyrocapsa* (3-4 µm) of Pliocene age are assigned to this group. They show a sporadic occurrence in the lower upper Pliocene. A more continuous range was recorded from the uppermost Pliocene (Zone NN19a) into the Pleistocene.

Sphenolithus spp.

Remarks. *Sphenolithus abies* and *S. neobies* are grouped under this label.

Genus RETICULOFENESTRA Hay, Mohler, and Wade, 1966

Reticulofenestra dornicoides (Black and Barnes) Pujos-Lamy, 1985

Remarks. These specimens of *Reticulofenestra* (5-6 µm) of Pliocene age have a largely elliptical outline, small central area, and extinction lines strong-

ly curved toward the outer part of the coccolith. The lowest occurrence was generally recorded in Zone NN16.

ACKNOWLEDGMENTS

We thank Dr. S.W. Wise for helpful comments and reviews on this paper. The second author would also like to thank Professors N. Ciaranfi and S. Monechi for encouraging her year in residence at Florida State University. Samples were provided by NSF through the Ocean Drilling Program. This study was supported by USSAC funds; laboratory facilities were provided by NSF grant no. DPP 91-18480.

REFERENCES

- Bukry, D., 1973. Low-latitude coccolith biostratigraphic zonation. In Edgar, N.T., Saunders, J.B., et al., *Init. Repts. DSDP*, 15: Washington (U.S. Govt. Printing Office), 685-703.
- , 1975. Coccolith and silicoflagellate stratigraphy, northwestern Pacific Ocean, Deep Sea Drilling Project Leg 32. In Larson, R.L., Moberly, R., et al., *Init. Repts. DSDP*, 32: Washington (U.S. Govt. Printing Office), 677-701.
- Cita, M.B., and Gartner, S., 1973. Studi sul Pliocene e sugli strati al passaggio dal Miocene al Pliocene. IV. The stratotype Zanclean foraminiferal and nannofossil biostratigraphy. *Riv. Ital. Paleontol.*, 79:503-558.
- Gartner, S., 1977. Calcareous nannofossil biostratigraphy and revised zonation of the Pleistocene. *Mar. Micropaleontol.*, 2:1-25.
- Lohman, W.H., 1986. Calcareous nannoplankton biostratigraphy of the southern Coral Sea, Tasman Sea, and southwestern Pacific Ocean, Deep Sea Drilling Project Leg 90: Neogene and Quaternary. In Kennett, J.P., von der Borch, C.C., et al., *Init. Repts. DSDP*, 90: Washington (U.S. Govt. Printing Office), 763-793.
- Martini, E., 1971. Standard Tertiary and Quaternary calcareous nannoplankton zonation. In Farinacci, A. (Ed.), *Proc. 2nd Int. Conf. Planktonic Microfossils Roma*: Rome (Ed. Tecnosci.), 2:739-785.
- Martini, E., and Müller, C., 1986. Current Tertiary and Quaternary calcareous nannoplankton stratigraphy and correlations. *Newsl. Stratigr.*, 16:99-112.
- Matsuoka, H., and Okada, H., 1989. Quantitative analysis of Quaternary nannoplankton in the subtropical northwestern Pacific Ocean. *Mar. Micropaleontol.*, 14:97-118.
- , 1990. Time-progressive morphometric changes of the genus *Gephyrocapsa* in the Quaternary sequence of the tropical Indian Ocean, Site 709. In Duncan, R.A., Backman, J., Peterson, L.C., et al., *Proc. ODP, Sci. Results*, 115: College Station, TX (Ocean Drilling Program), 255-270.
- Okada, H., and Bukry, D., 1980. Supplementary modification and introduction of code numbers to the low-latitude coccolith biostratigraphic zonation (Bukry, 1973; 1975). *Mar. Micropaleontol.*, 5:321-325.
- Perch-Nielsen, K., 1985. Cenozoic calcareous nannofossils. In Bolli, H.M., Saunders, J.B., and Perch-Nielsen, K. (Eds.), *Plankton Stratigraphy*: Cambridge (Cambridge Univ. Press), 427-554.
- Pujos, A., 1985. Quaternary nannofossils from Goban Spur, eastern North Atlantic Ocean, Deep Sea Drilling Project Holes 548 and 549A. In de Graciansky, P.C., Poag, C.W., et al., *Init. Repts. DSDP*, 80: Washington (U.S. Govt. Printing Office), 767-792.
- Raffi, I., Backman, J., Rio, D., and Shackleton, N.J., 1993. Plio-Pleistocene nannofossil biostratigraphy and calibration to oxygen isotopes stratigraphies from Deep Sea Drilling Project Site 607 and Ocean Drilling Program Site 677. *Paleoceanography*, 8:387-408.
- Raffi, I., and Rio, D., 1979. Calcareous nannofossil biostratigraphy of DSDP Site 132—Leg 13 (Tyrrhenian Sea-Western Mediterranean). *Riv. Ital. Paleontol. Stratigr.*, 85:127-172.
- Rio, D., Fornaciari, E., and Raffi, I., 1990a. Late Oligocene through early Pleistocene calcareous nannofossils from western equatorial Indian Ocean (Leg 115). In Duncan, R.A., Backman, J., Peterson, L.C., et al., *Proc. ODP, Sci. Results*, 115: College Station, TX (Ocean Drilling Program), 175-235.
- Rio, D., Raffi, I., and Villa, G., 1990b. Pliocene-Pleistocene calcareous nannofossil distribution patterns in the Western Mediterranean. In Kastens, K.A., Mascle, J., et al., *Proc. ODP, Sci. Results*, 107: College Station, TX (Ocean Drilling Program), 513-533.

- Sato, T., and Takayama, T., 1992. A stratigraphically significant new species of the calcareous nannofossil *Reticulofenestra asanoi*. In Ishizaki, K., and Saito, T. (Eds.), *Centenary of Japanese Micropaleontology*: Tokyo (Terra Sci. Publ.), 457-460.
- Takayama, T., and Sato, T., 1987. Coccolith biostratigraphy of the North Atlantic Ocean, Deep Sea Drilling Project Leg 94. In Ruddiman, W.F., Kidd, R.B., Thomas, E., et al., *Init. Repts. DSDP*, 94 (Pt. 2): Washington (U.S. Govt. Printing Office), 651-702.
- Wei, W., 1993. Calibration of upper Pliocene-lower Pleistocene nannofossil events with oxygen isotope stratigraphy. *Paleoceanography*, 8:85-99.
- Wei, W., Bergen, J.A., and Applegate, J., 1988. Cenozoic calcareous nannofossils from the Galicia Margin, Ocean Drilling Program Leg 103. In Boillot, G., Winterer, E.L., et al., *Proc. ODP, Sci. Results*, 103: College Station, TX (Ocean Drilling Program), 279-292.

Date of initial receipt: 1 December 1994

Date of acceptance: 21 August 1995

Ms 149SR-209

APPENDIX

Alphabetic List of Taxa

- Amaurolithus delicatus* Gartner and Bukry, 1975
Amaurolithus tricorniculatus (Gartner) Gartner and Bukry, 1975
Calcidiscus leptoporus (Murray and Blackman) Loeblich and Tappan, 1978
Calcidiscus macintyreii (Bukry and Bramlette) Loeblich and Tappan, 1978
Ceratolithus cristatus Kamptner, 1950
Coccolithus pelagicus (Wallich) Schiller, 1930
Dictyococcites perplexa Barnes, 1975
Dictyococcites productus (Kamptner 1963) Backman, 1980
Discoaster asymmetricus Gartner, 1969
Discoaster brouweri Tan, emend. Bramlette and Riedel, 1954
Discoaster challengerii Bramlette and Riedel, 1954
Discoaster intercalaris Bukry, 1971
Discoaster pentaradiatus Tan, emend. Bramlette and Riedel, 1954
Discoaster surculus Martini and Bramlette, 1963
Discoaster tamalis Kamptner, 1967
Discoaster triradiatus Tan, 1927
Discoaster variabilis Martini and Bramlette, 1963
Emiliana huxleyi (Lohmann, 1902) Hay and Mohler, 1967
Geminolithella rotula (Kamptner) Backman, 1980
Gephyrocapsa caribbeanica Boudreaux and Hay, 1969
Gephyrocapsa oceanica Kamptner (1943)
Helicosphaera acuta Theodoridis, 1984
Helicosphaera carteri (Wallich) Kamptner, 1954
Helicosphaera sellii Bukry and Bramlette, 1969
Helicosphaera wallichii (Lohmann) Boudreaux and Hay, 1969
Oolithotus fragilis (Lohmann) Martini and Müller, 1972
Pontosphaera anisotrema (Kamptner) Backman, 1980
Pontosphaera discopora Schiller (1925)
Pontosphaera japonica (Takayama) Nishida, 1971
Pseudoemiliana lacunosa (Kamptner) Gartner, 1969
Reticulofenestra asanoi (Sato and Takayama), 1992
Reticulofenestra daronicoides (Black and Barnes) Pujos, 1985
Reticulofenestra gelida (Geitzenauer) Backman, 1978
Reticulofenestra minuta Roth, 1970
Reticulofenestra minutula (Gartner) Haq and Berggren, 1978
Reticulofenestra pseudoumbilicus (Gartner) Gartner, 1969
Rhabdosphaera claviger Murray and Blackman, 1898
Syracosphaera pulchra Lohmann, 1902
Scapholithus fossilis Deflandre, 1954
Sphenolithus abies Deflandre, 1954
Sphenolithus neoabies Bukry and Bramlette, 1969
Umbilicosphaera sibogae foliosa (Kamptner) Okada and McIntyre, 1977

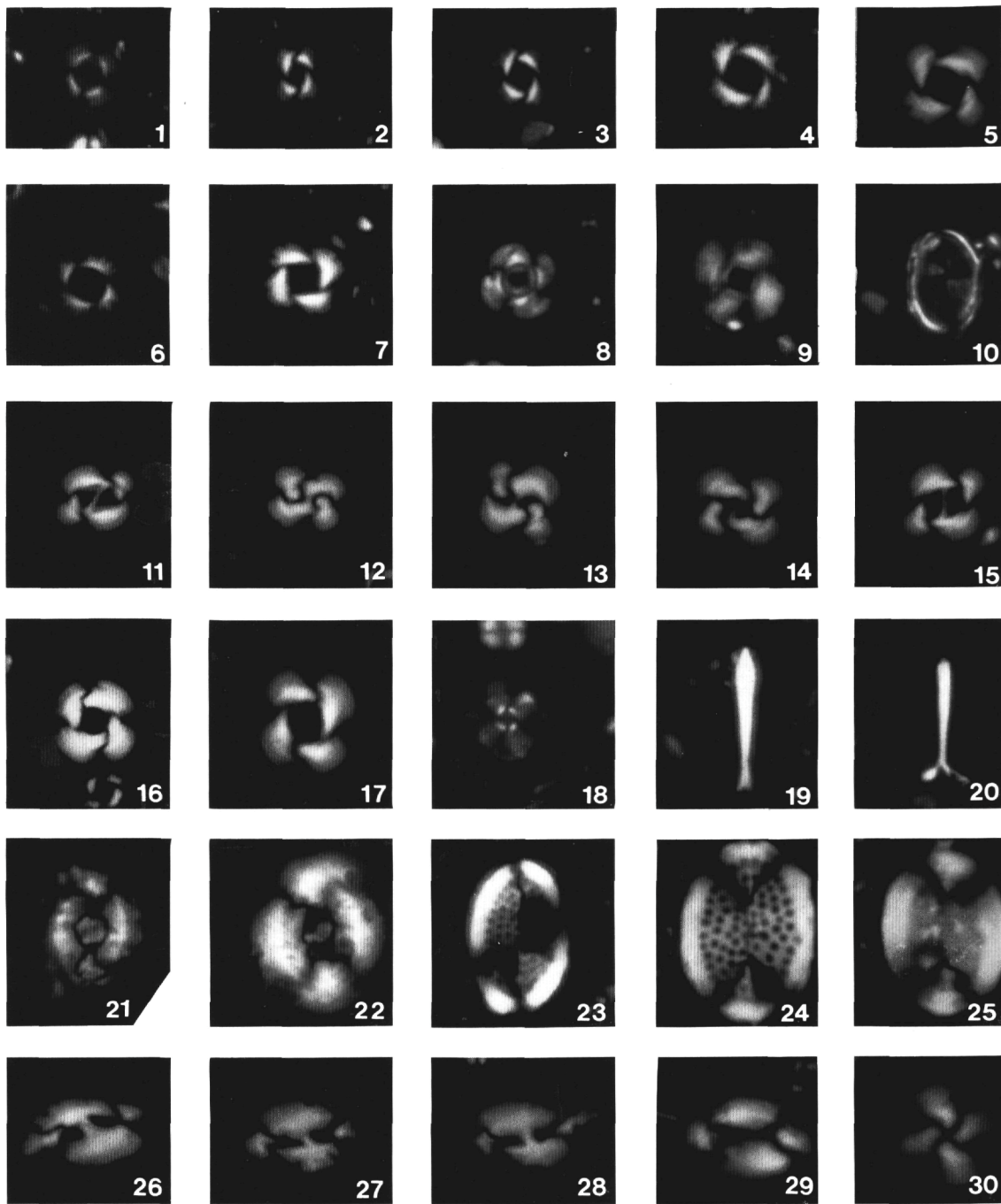


Plate 1. All illustrations are light micrographs. The abbreviation pol denotes polarized light. The magnification for all Plate 1 figures is 2500× except Figure 16 (2000×). **1-3.** *Emiliana huxleyi*, Sample 149-898A-1H-1, 2-3 cm, pol. **4-7.** *Pseudoemiliana lacunosa*, Sample 149-898A-6H-2, 67-68 cm, pol. **8, 9.** *Umbilicosphaera sibogae*, Sample 149-898A-11H-2, 17-18 cm, pol. **10.** *Syracosphaera pulchra*, Sample 149-898A-1H-2, 54-55 cm, pol. **11.** *Gephyrocapsa oceanica* s.l., Sample 149-898A-11H-2, 17-18 cm, pol. **12.** *Dictyococcites perplexa*, Sample 149-898A-11H-2, 17-18 cm, pol. **13.** *Gephyrocapsa caribbeanica* (>5.5 μm), Sample 149-898A-11H-2, 17-18 cm, pol. **14, 15.** *Gephyrocapsa oceanica* (>5.5 μm), Sample 149-898A-11H-2, 17-18 cm, pol. **16, 17.** *Reticulofenestra asanoi*, Sample 149-898A-6H-2, 67-68 cm, pol. **18.** *Umbellosphaera irregularis*, Sample 149-898A-16X-1, 83-84 cm, pol. **19, 20.** *Rhabdosphaera claviger*, Sample 149-898A-6H-2, 67-68 cm, pol. **21, 22.** *Coccolithus crassipons*, Sample 149-898A-11H-2, 17-18 cm, pol. **23, 24.** *Pontosphaera discopora*, Sample 149-898A-11H-2, 17-18 cm, pol. **25.** *Pontosphaera japonica*, Sample 149-898A-11H-2, 17-18 cm, pol. **26-28.** *Helicosphaera sellii*, Sample 149-898A-14H-1, 141-142 cm, pol. **29.** *Helicosphaera carteri*, Sample 149-898A-6H-2, 67-68 cm, pol. **30.** *Calcidiscus leptoporus*, Sample 149-898A-11H-2, 17-18 cm, pol.

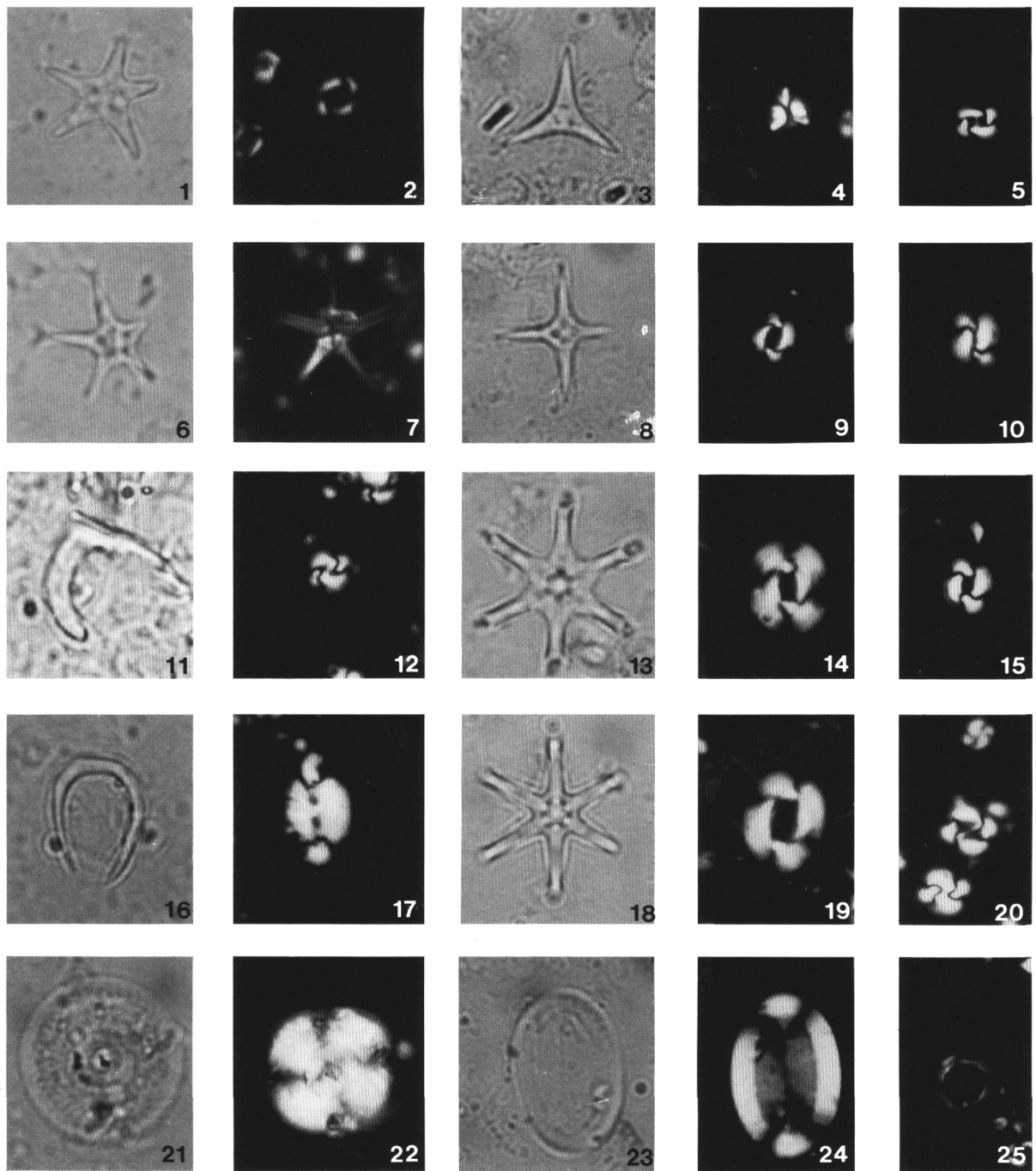


Plate 2. All illustrations are light micrographs. The abbreviations pol and tr denote polarized and transmitted light, respectively. The magnification for all Plate 2 figures is 2000 \times except Figure 2 (2500 \times). **1.** *Discoaster asymmetricus*, Sample 149-899A-6R-2, 104-105 cm, tr. **2.** *Pseudoemiliana lacunosa*, Sample 149-900A-11R-4, 119-120 cm, pol. **3.** *Discoaster triradiatus*, Sample 149-899A-6R-1, 78-79 cm, tr. **4.** *Sphenolithus* spp., Sample 149-900A-11R-4, 119-120 cm, pol. **5.** *Gephyrocapsa parallela*, Sample 149-898A-5H-4, 30-31 cm, pol. **6, 7.** *Discoaster pentaradiatus*, Sample 149-899A-7R-1, 40-41 cm, (6, tr; 7, pol). **8.** *Discoaster tamalis*, Sample 149-899A-6R-1, 78-79 cm, tr. **9.** *Reticulofenestra minutula*, Sample 149-897C-26R-1, 71-72 cm, pol. **10.** *Dictyococcites perplexa*, Sample 149-899A-6R-4, 40-41 cm, pol. **11.** *Amaurolithus tricorniculatus*, Sample 149-899A-7R-1, 81-82 cm, tr. **12.** *Gephyrocapsa caribbeanica*, Sample 149-900A-6R-3, 86-87 cm, pol. **13.** *Discoaster surculus*, Sample 149-900A-11R-4, 119-120 cm, tr. **14.** *Reticulofenestra gelida*, Sample 149-899A-6R-4, 40-41 cm, pol. **15.** *Reticulofenestra doronicoides*, Sample 149-900A-7R-1, 17-18 cm, pol. **16.** *Amaurolithus delicatus*, Sample 149-899A-6R-4, 40-41 cm, tr. **17.** *Helicosphaera acuta*, Sample 149-900A-7R-1, 17-18 cm, pol. **18.** *Discoaster brouweri*, Sample 149-899A-5R-1, 72-73 cm, tr. **19.** *Reticulofenestra pseudoumbilicus*, Sample 149-899A-6R-4, 40-41 cm, pol. **20.** *Gephyrocapsa oceanica* s.l., Sample 149-898A-15X-5, 14-15 cm, pol. **21, 22.** *Calcidiscus macintyreii*, Sample 149-899A-2R-2, 52-53 cm, (21, tr; 22, pol). **23, 24.** *Pontosphaera japonica*, Sample 149-899A-2R-2, 52-53 cm, (23, tr; 24, pol). **25.** *Geminilithella rotula*, Sample 149-900A-11R-4, 119-120 cm, pol.